Wind turbine power performance testing using a Lidar

A field study

MSc thesis
H.C. (Henrik) van der Velde[a]

February 26, 2016

Supervisors:
Drs. J.P. (Jan) Coelingh[b]
Dr. W.G.J.H.M. (Wilfried) van Sark[c]
Dr. ir. W.A.A.M. (Wim) Bierbooms[d]
Second reader:
Msc. B. (Boudewijn) Elsinga[e]

[a] henrikvdv@gmail.com
[b] Wind&Site, Nuon, part of Vattenfall
[c] Copernicus Institute of Sustainable Development, Utrecht University
[d] Wind Energy, Delft University of Technology
[e] Energy Science, Utrecht University

Summary

In recent years, the installed capacity of wind turbines has increased rapidly, thereby raising the stakes for wind turbine power performance testing. The current standard for power performance testing, IEC 61400-12-1, prescribes to measure the wind speed at hub height using a meteorological mast. This study tested whether Lidar, a remote measurement technology, could improve power performance testing. Potential benefits include mobility of the measurement device and increased insight in wind speed, with measurements up to approximately 200 meter height.

A measurement campaign was held at a site with flat terrain by positioning a ZephIR 300 Lidar next to an IEC compliant meteorological mast to measure the power performance of two wind turbines. Wind speed measurements were compliant to Norsewind criteria with a linear regression slope of 0.989 indicating that the Lidar measured lower wind speeds than the meteorological mast. Three major conclusions were drawn. (I) The difference in wind speed measurement has a large effect on annual energy production estimation (2.5 % for a Rayleigh function with a mean annual wind speed of 7 m/s), but difference in power performance of two wind turbines was found by either using the meteorological mast or the Lidar. (II) The rotor equivalent wind speed approach reduced scatter in the power curve for the Lidar compared to hub height wind speed, but not compared to hub height wind speed measurement by the meteorological mast. (III) Inner- and inner+outer envelope guaranteed power curve conditions showed a difference in annual energy production of approximately 1 % for a Rayleigh function with a mean annual wind speed of 7 m/s.

The most important implications are the following. (I) It is advized to use a Lidar to compare the power performance of multiple wind turbines or to use it for comparing performance over time, but it is advised not compare power performance measured for one test with a Lidar and for another test using a meteorological mast. (II) For power performance guarantee negotiations Lidar measurements could be included as option for power performance measurement and with REWS calculations the inner envelop conditions could be enlarged, but a different guaranteed power curve than when measured using a meteorological mast might be needed. (III) For flat terrain with grassland and wind turbines of approximately 100 meter hub height, rotor equivalent wind speed and veer calculations are not adding much insight and are not needed for inclusion in the power performance testing, except when used for extending inner envelope conditions.

Keywords: Wind energy, power performance testing, Wind Doppler Lidar, rotor equivalent wind speed, wind veer, power curve guarantee.

Acknowledgements

Contents

List of Figures

List of Tables

Chapter 1

Introduction

Currently, renewable energy sources account only for a small share of the world total energy supply (Figure 1.1). However, with depleting fossil energy resources, energy security needs and climate change problems, renewables are becoming increasingly important. This trend reflected in a large growth rate for wind energy as depicted in Figure 1.2.
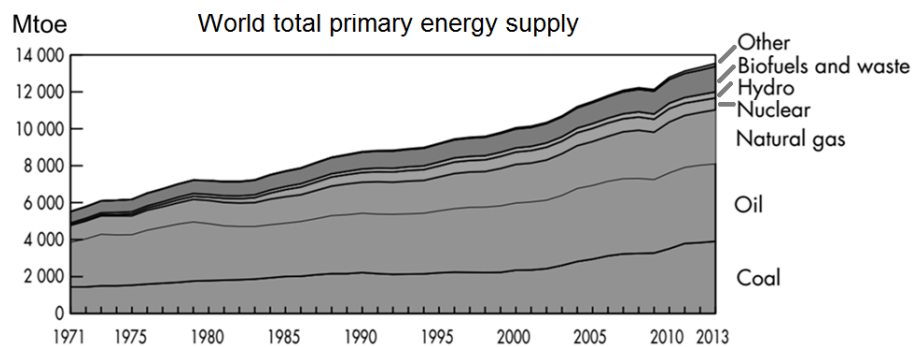
Figure 1.1: World energy supply in million tonnes of oil equivalent (IEA, 2015). The category "other" consists of geothermal, solar, wind, heat and others.
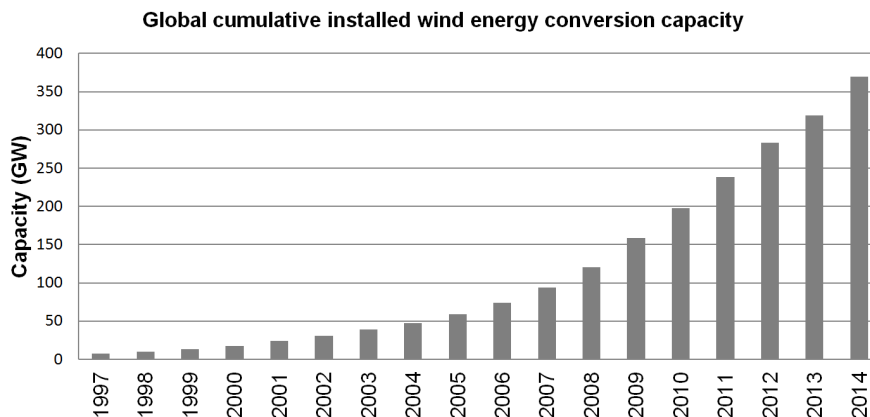
Figure 1.2: Global cumulative installed capacity of wind turbines (GWEC, 2014).

Having a good understanding on the power performance of a wind turbine is of key importance for wind energy projects and becoming increasingly important due to the increasing installed capacity of wind turbines. The power performance is defined as the fraction of energy in the wind that is converted to electricity. The key performance parameter of a wind turbine is its power curve, which describes the power output as function of wind speed. The power curve is used for both pre-construction and post-construction analysis. In pre-construction analysis the power curve can be combined with the estimated wind speed distribution at a site to calculate the expected annual energy production of a wind turbine at a specific location. In post-construction analysis the contracted power curve can be compared to the actual power curve to see whether the turbine is performing according to the guaranteed power curve and if not, it can be tried to adjust parameters such as the pitch angle of the blades or yaw angle of the nacelle to improve the performance.

It is not straight-forward to calculate the power performance of a wind turbine (Figure 1.3). Firstly, the wind speed at nacelle of a wind turbine itself can not be used for power performance calculation. This is because the wind is slowed down by the wind turbine. If the wind turbine is trying to extract too much energy, the wind is slowed down too much so that the wind turbine does not obtain all energy that would be available when trying to extract less energy. Secondly, there can be non-uniform wind speed conditions, for example the wind speed and wind direction can differ over space and height.

In order to construct consistent and comparable power curves, the IEC 2005 power performance standard is used industry-wide. The current IEC 61400-12-1 standard is dated 2005 (IEC, 2005).

However, since 2005 new developments lead to the need and possibility to improve this standard. Therefore the IEC is proposing a new standard, the IEC 61400-12-1 Edition 2 (IEC, 2015). The current IEC standard prescribes to measure the wind speed at hub height, which reduces height and cost of meteorological masts at the measurement location (Figure 1.4). However, the diameter of wind turbine rotors is increasing (IEA, 2013). Therefore the wind speed and wind direction at hub height are becoming less representative for the wind conditions over the whole rotor area (EWEA, 2009; Wharton and Lundquist, 2012). To encounter this problem, the rotor equivalent
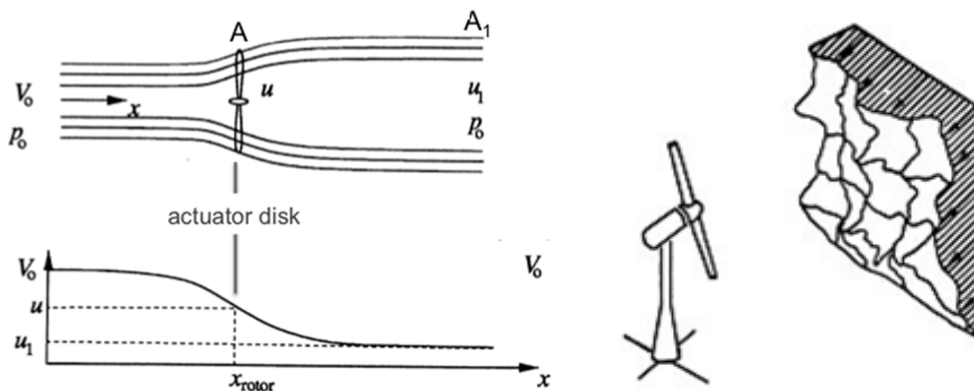
Figure 1.3: Complexity of power performance testing with the actuator disc theory (Hansen, 2015) and spatial wind speed variation (TU Delft, 2016).

wind speed approach has been developed where the wind speed at multiple heights is taken into account and translated to a representative (rotor equivalent) wind speed in order to make more reliable power curves for large wind turbines (Wagner et al., 2011). This approach is suggested in the second edition standard of the widely used IEC power performance standard (IEC, 2015). Furthermore the IEC 2005 standard prescribes to measure the wind speed with anemometers at a meteorological mast. Currently, a meteorological mast often only measures up to hub height of a wind turbine.

Recently, as an alternative to meteorological masts, Lidar remote sensing technology has emerged. Reason include its mobility and its ability of remote measurements up to heights of 200 meter above ground level as illustrated in Figure 1.4 (Mann et al., 2008). A Lidar measures the wind velocity by analyzing the Doppler-shift of a laser beam reflected by aerosols (Smith et al., 2005). The use of Lidars for power performance tests is described in the proposed second edition IEC standard.

Studies show that Lidars can measure the wind speed with a high accuracy at flat terrain (Mann et al., 2008; Smith et al., 2005). The IEC proposes to allow for Lidar measurements in some situations, when a small meteorological mast is accompanying the Lidar (IEC, 2015). The meteorological mast enables lidar validation and can measure fast fluctuations around the 10-minute mean wind speed(turbulence).

Multiple studies analyzed the power performance test standards. Wagner et al. (2014) tested the rotor equivalent wind speed approach at one site for a 500 kW wind turbine. However, it faced insignificant influence of wind shear (changing wind speed with height). For the other sites, only the difference in estimated power output had been analyzed and not the real power output. Wächter et al. (2009) measured the wind speed at hub height with a meteorological mast and a Lidar at flat terrain and concluded that the power curves obtained after one month were in good correspondence. The Lidar was not validated against the mast. Antoniou et al. (2009) concluded a year long measurement campaign with the notion that the rotor equivalent wind speed approach is recommended (Dupont et al., 2012). Westerhellweg et al. (2010) showed that at an offshore site, the
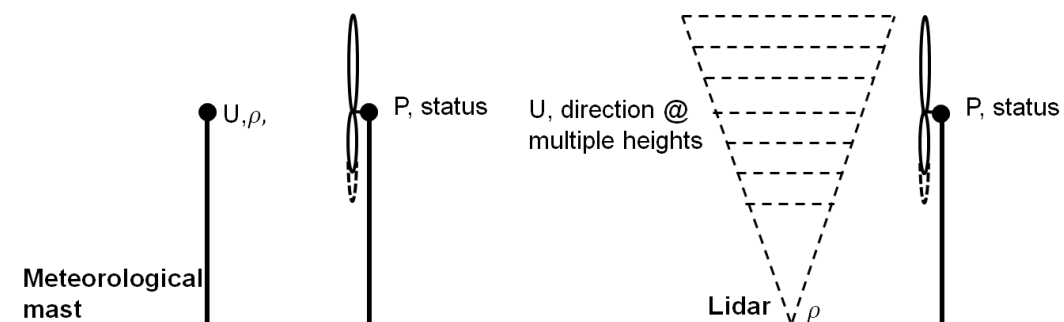
Figure 1.4: Power performance testing using meteorological mast in front of a wind turbine according to IEC 2005 (left), and using a Lidar (right).

rotor equivalent wind speed approach improved the power performance test.

Whereas these studies show that the wind speed measurements with a Lidar can be measured well compared to a meteorological mast, it is unclear what the effect is on power performance testing. In other words, how much does it matter that a Lidar does not measure exactly the same wind speed as a meteorological mast. Also, it remains unclear whether it would be recommended to use a rotor equivalent wind speed approach for power performance testing. Moreover, it remains unclear how much the impact is for having power performance guarantees on only some inner envelope conditions, as opposed to when a guarantee would hold for all conditions that could be measured for an IEC compliant power performance test.

The aim of this study is to improve the insight in power performance testing and to find out what the added value is when using a Lidar. The following questions are posed, including an elaboration on its implications:

1. What are the site conditions during the measurement campaign?

    - To get a feeling for the generalization of the results to other projects.

2. How well do the Lidar measurements compare to measurements of sensors at the meteorological mast?

    - The key issue for the use of a Lidar is how its measurements compare to those of the currently widely accepted sensors at the meteorological mast.

3. How large is the relative difference of annual energy production calculations between measuring with a meteorological mast and measuring with a Lidar? What are the causes for that difference?

    - If there are no large differences after applying corrections, then the Lidar can be used for measuring the power performance at other turbines.

    - Also the insight can be used for future wind turbine performance contracts, to negotiate that the measurements with a ZephIR 300 are suitable for the power performance verification.

4. To test the added value of rotor equivalent wind speed and veer calculations that can be applied using a Lidar, the following questions are posed: How much does the scatter around the power curve reduce when applying corrections for rotor equivalent wind speed and veer? And what is the difference in calculated annual energy production?

    - If the scatter reduces we can improve monitoring the turbines and better understand why turbines at certain moments perform better or worse.

    - Also the insight can be used for negotiating this option for future power performance contracts of wind turbines.

5. To get more insight on the effect of inner- and outer envelope conditions of a power performance guarantee: What percentage of time do inner-envelope conditions occur? And what

is the annual energy production difference for inner- and outer- envelope conditions of the guaranteed power curve?

- To understand the impact of the power curve contract and to understand how often there is no contracted performance.

- To get insight for future negations whether the current approach is appropriate or that there should also be some guarantee for outer-envelope conditions.

6. For understanding the impact of invalid measurements by the Lidar: Are errors and outages of the Lidar systematically occurring during certain meteorological conditions?

- This could delay the measurement campaigns for power performance testing.

- This could give erroneous estimations when a Lidar is used for estimating the mean wind speed at a site.

This study is performed at Vattenfall where wind farms are developed, constructed and operated. The results of this study could contribute to a better understanding of the applicability of the new power performance standard, and the use of Lidar technology. When it would be concluded that the Lidar can measure the power curve as well as or better than a meteorological mast, then this could lead to using the Lidar at multiple turbines to quickly find out wrong settings. Additionally it could lead to deployment of Lidars at green fields to measure the wind resource without having to install a meteorological masts.

Chapter 2

Theoretical background

In the following sections, first the working principle of a Lidar will be explained followed by the specifications of the ZephIR 300 Lidar as used in this research. Thereafter IEC 61400-12-1 Edition 1 and proposed IEC 61400-12-1 Edition 2 power performance standards will be elaborated on.

2.1 Doppler Wind Lidar

2.1.1 Working principle

Lidar is a remote measurement technology that can be used to measure the wind speed at multiple heights (Figure 2.1). Light is emitted at a source and its radiation is partially scattered back on a receiver (Figure 2.2). The signal is processed by software to measure the distance to an object or to measure the velocity of an object. Lidar technology is used in multiple applications including mapping the earth's service with a Lidar in plane, but can also be used to measure the wind speed and wind velocity. For wind measurements it is not only important to measure the wind speed but also the distance at which the measured speed holds.

With wind speed being the collective movement of air, is measured by a Wind Doppler Lidar. Air consists of air particles (mainly nitrogen and oxygen) on the one hand, and aerosols on the other hand. Aerosols are small solid or fluid particles in the air, typically dust, water droplets, pollution, pollen or salt crystals (Smith et al., 2005). A Wind Doppler Lidar can be used for measuring wind speed and wind direction at a distance from the device. These devices often are used for scanning up to multiple heights (Figure 2.1), but can also be placed atop a nacelle of a wind turbine to measure the wind speed at multiple distances in front of a wind turbine. A Wind Doppler Lidar measures the wind speed using the Doppler effect. The Doppler effect is more widely known from sound but can also be used for electromagnetic radiation such as X-ray and light. The Doppler effect theory states that the frequency of emitted radiation as perceived by an observer changes when the velocity of the emitting source from or towards the observer changes. When measuring the Doppler shift of light, the following equation holds for the calculating the velocity v of an

(a) Illustration (Smith et al., 2005)

(b) Lidar at the test site, seen from the top
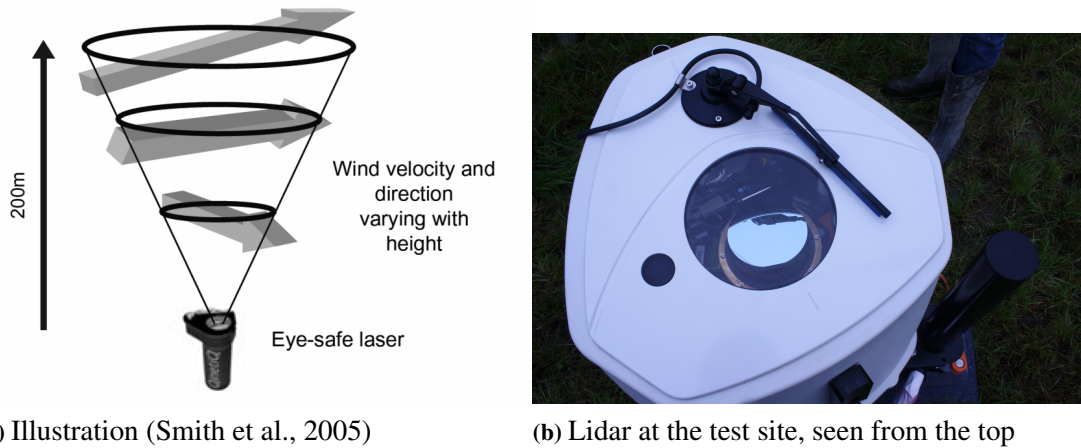
Figure 2.1: ZephIR 300 in ground based upward-looking mode
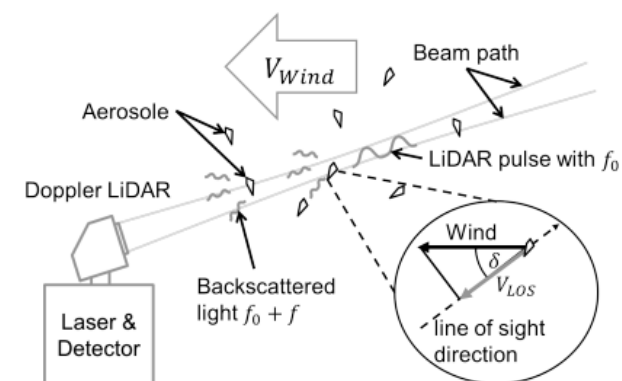
Figure 2.2: Working principle of Lidar wind measurements adapted from Hieronimus (2015).

object that is emitting radiation (the specific form of the general Doppler formula holds because the speed of light is not "advected" by some medium. In other words, the speed of the wave traveling through the medium does not change with the properties of the medium).

$$f = f_0(1 + v/c) \tag{2.1}$$

Where

f is the frequency of the received signal;

f_0 is the frequency of the emitted signal;

v is the speed of the object in the line of sight;

c is the speed of light.

An particle that was illuminated by a Lidar would observe the Light with a frequency as in Equation 2.1. The radiation that is scattered back with that frequency would be observed by the receiver at the Lidar with again a frequency shift. Therefore the following equation holds.

$$f = f_0 + \Delta f = f_0(1 + 2v/c) \tag{2.2}$$

Where Δf is the frequency difference between sent and received signal of the Lidar.

It should be noted that for wind speed measurements the sensitivity of a Lidar has to be high, as the ratio between the speed of the object and the speed of light is really small, e.g. for a wind speed of 3 m/s, the ratio is $3/(3 * 10^8) = 1/10^8$. Not only do the particles move collectively in a direction which is observed as wind speed, also do the particles vibrate and increasingly with increasing temperature. These movements have a higher speed than the wind speed (Weitkamp and Wandinger, 2005). Also these movements are observed by a Wind Doppler Lidar. Aerosols have a lower speed with temperature than air particles do, so that the wind speed can be measured more easily when these particles are present in the air (Weitkamp and Wandinger, 2005). Figure 2.3 illustrates the difference in signal obtained from the measurements when aerosols are present versus not present.
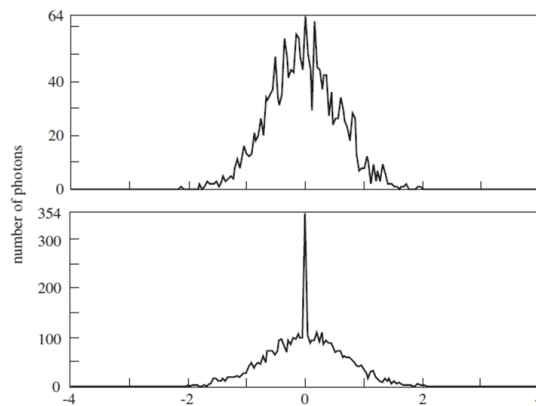
Figure 2.3: Illustration on the measured signal when no aerosols are present (above), and when aerosols are present (below). Adapted from Weitkamp and Wandinger (2005)

.

(a) Installation

(b) Installed, with meteorological station at the top left
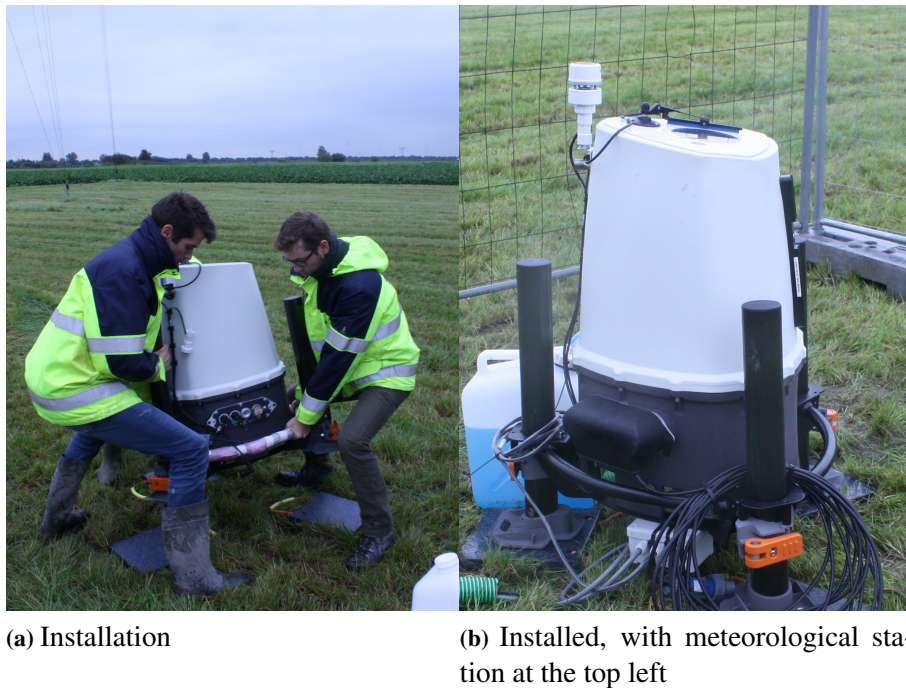
Figure 2.4: ZephIR 300.

Only the line of sight speed of an object can be measured using Doppler. However, wind speed information is requested in the horizontal direction and including the wind direction, thus extra information has to be added. Options are to install multiple Lidars focused at one point or to measure multiple points close to each other with one Lidar on a different angle. For this second option Lidars exist with multiple beams (e.g. the Leosphere WindCube) or one moving beam (e.g. the ZephIR 300, Section 2.1.2).

2.1.2 ZephIR 300

A ZephIR 300 was used in this research (Figure 2.4). The ZephIR 300 is a type of Wind Doppler Lidar and has the following specifications. The measurement height of the ZephIR 300 is approximately 10 to 200 meter above ground level. The type used for this research is a ZephIR 300 DM, where DM means dual mode. It can be installed at a nacelle to scan the wind field in front of a wind turbine, but here was used to measure the wind field above the Lidar. This lidar transmits light at a wavelength of $1.55\,\mu m$ which can not penetrate nor harm the human eye (because wavelength $> 1.4\,\mu m$ (Jaynes et al., 2007)). The ZephIR 300 is a continuous wave Doppler Lidar which as its name suggests emits radiation continuously, in contrast to a pulsed Lidar. A major advantage of a continuous wave Lidar is that it can be easier and cheaper to build than a pulsed Lidar. For a continuous wave Lidar, it can not be timed how far the measured object is away from the Lidar. Therefor the beam is focused using a telescope. The measurement height of the can be adjusted using the focus of the telescope. When differing the focus not only the distance is adjusted, but also the length of the focus area is changed. When the focus distance x from the Lidar is chosen,

(a) Side view   **(b)** Top view
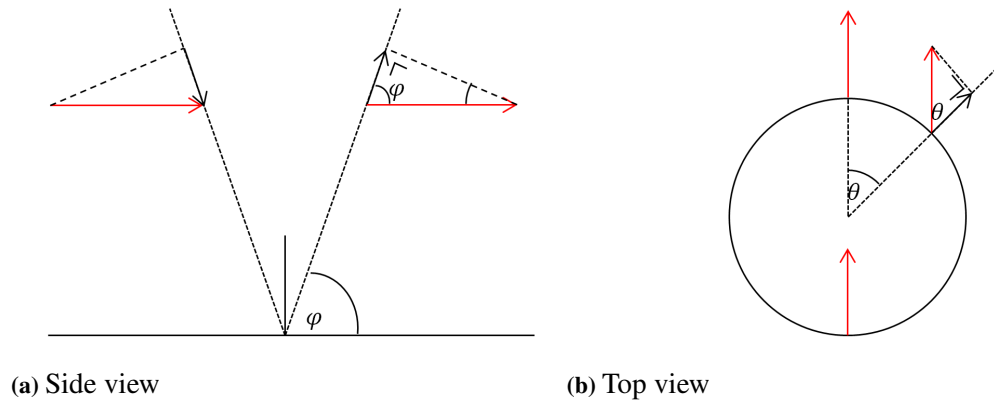
Figure 2.5: Horizontal wind speed and wind direction deduction from line of sight windspeed (u_{los}) measurements.

the length of the depth range can be calculated as follows (Weitkamp and Wandinger, 2005).

$$\Delta x = \frac{4x^2 \lambda}{A} \tag{2.3}$$

Where
Δx is the probed depth;
x is the focus distance;
λ is the wave length of the laser;
A is the area of the receiver.

Thus, the focus area enlarges when the focus is further away from the Lidar. For the ZephIR 300, the focus area is approximately 0.07 m at 10 meter height and 7.70 meter at 100 meter height (ZephIR, 2015c). For filtering the signal at the receiver, the ZephIR 300 uses coherent detection which is a form of heterodyne detection. Basically the received signal with frequency f_1 and a sent signal with frequency f_2 are mixed creating two new signals with frequency $f_1 + f_2$ and $f_1 - f_2$. The signal with the difference in frequency is measured by the detector and can be measured to high accuracy because the frequency is low. Also the sign of the difference in frequency is measured (Weitkamp and Wandinger, 2005, p.337) .

For obtaining the wind speed information not only in the line of sight of the laser, the beam is scanning a cone. The horizontal wind speed and wind direction can be deducted from the line of sight (LOS) velocity using trigonometry as illustrated in Figure 2.5. With the line of sight velocity, the horizontal wind speed can be calculated using the elevation angle ϕ. At multiple azimuth angles the wind speed in the line of sight is measured in this so called Velocity Azimuth Display (VAD) method. The ZephIR 300 scans one height first, using approximately 1 second. During one rotation 50 points are scanned (ZephIR, 2015a). The wind velocity **u** can be interpreted using the line of sight wind velocity and azimuth angle (illustrated in Figure 2.7) with the next equation.
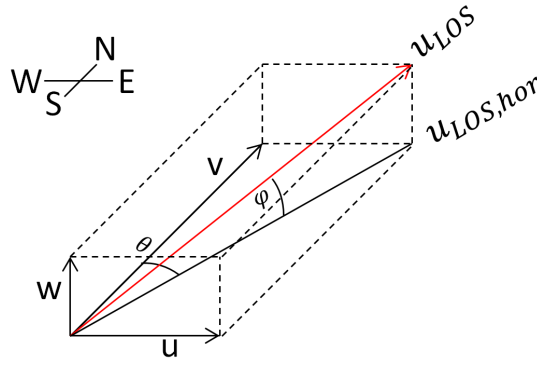
Figure 2.6: Line of sight wind speed for given wind velocity vector and azimuth angle and elevation angle.
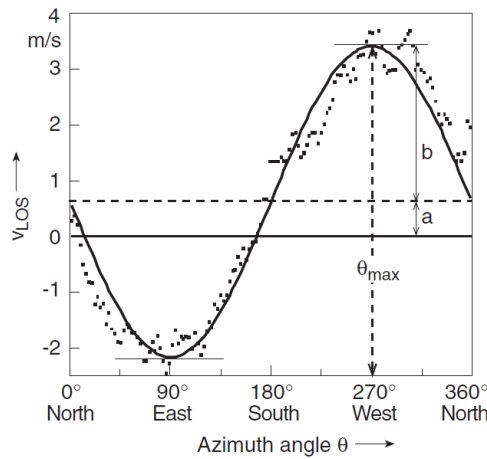
Figure 2.7: Output of the VAD scan (Weitkamp and Wandinger, 2005).

$$\mathbf{u} = (u, v, w) = \left(\frac{b \sin(\theta_{max})}{\cos(\phi)}, \frac{b \cos(\theta_{max})}{\cos(\phi)}, \frac{a}{\sin(\phi)} \right) \tag{2.4}$$

Where

u is the West–East wind velocity component;

v is the South–North wind velocity component;

w is the vertical wind velocity component;

θ is the clockwise azimuth angle, starting from the North;

ϕ is the is the elevation angle (the angle between the horizontal plane and the angle of the laser);

the other parameters are illustrated in Figure 2.7.

Equation 2.4 is derived in Section A.

One extra complexity needs to be overcome for the ZephIR software to determine the wind direction. The line of sight velocity is measured in absolute terms, but the direction of the line of sight velocity can not be determined. A part of the sent signal (from the local oscillator) is used
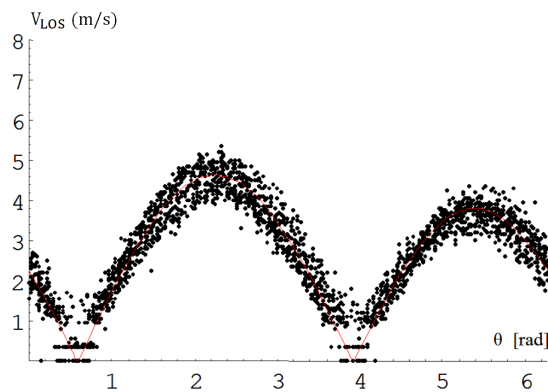
Figure 2.8: Output of VAD scan for homodyne Lidar systems (Danielian et al., 2006).

as reference signal in the receiver to determine the difference between the backscattered and sent signal frequency. Techniques where the sign of the difference can be measured exist, these are heterodyne systems. However, the ZephIR 300 uses homodyne detection, where the sign can not be determined because the local oscillator is not shifted in frequency (Courtney et al., 2008; Mann et al., 2010). A major advantage of this setup is that it is cheaper. However, the output of the VAD scan (Figure 2.7) is only seen in as Figure 2.8, and the wind direction is at one of the two maxima. This ambiguity is resolved by using the wind direction measurements of the meteorological station mounted at the Lidar (Courtney et al., 2008).

2.1.3   Lidar performance according to literature

The performance of Lidars has been validated against anemometers at the meteorological masts. At flat terrain the correlation between Lidar and anemometer wind speed can be $\geq 99\%$ (Mann et al., 2008; Smith et al., 2005). Offshore, Pena et al. (2009) observed correlations between 90% and 96% while Westerhellweg et al. (2010) observed correlations as high as 99%. At complex terrain a Lidar might perform insufficiently for wind speed measurements, due to the lack of horizontal homogeneity of the flow, which is assumed for the interpretation of lidar data (Bingöl et al., 2009).

The largest uncertainties are introduced by two causes. Firstly by measuring at the intended measurement height. Secondly by interpolating the wind speed from the measurements at some points along the circle for which often the assumption is made that the wind velocity along three axis is constant over the plane. For complex terrains this is not a valid assumption. Generally, the uncertainties are influenced by hardware issues and atmospheric conditions including rain and clouds. Cloud correction algorithms are used to reduce uncertainties when clouds are present. A detailed analysis of factors influencing Lidar measurements is provided by Lindelöw-marsden (2009).

Table 2.1: Studies comparing met mast and lidar power curve with the abreviations [y] yes, [n] no, [-] not mentioned and [EAEP] estimated annual energy production. The duration of the measurement campaign can be found under months. The regression coefficiënt is shown under validated, where the wind speed of the lidar and met mast are compared to each other. Mast indicates the heighest measurment of the wind speed at the mast.

Nr.	Research	Lidar	Terrain	Months	Validated	REWS
1	Wächter et al. (2009)	Windcube	Flat	1	n	n
2	Dupont et al. (2012)	Leosphere WLS7	Flat	4	R^2 0.996	y
3	RES (2014)	ZephIR DM	Flat	-	R^2 0.999	y
4	Antoniou et al. (2009)	Windcube	Flat	12	n	y
5	Wagner et al. (2014)	Windcube	Offshore	-	n	y

Nr.	Conclusion	Mast (m)	hub (m)
1	Powercurve lidar in good correspondence with mast	102	102
2	REWS recommended	80	-
3	Distance lidar - turbine relative insensitive	-	-
4	REWS and turbulence intensity normalization recommended	116.5	80
5	Difference hub vs rews EAEP, not compared to power output	-	91

Nr.	Wind veer	Turbulence	IEC Ed. 2 method
1	n	n	-
2	n	n	-
3	n	n	-
4	n	n	-
5	n	n	y

2.2 Comparing power curves constructed using meteorological mast or lidar

A draft of the new IEC standard has been evaluated in an comparative exercise where eight organizations have implemented the IEC 61400-12-1 Ed. 2 Committee Draft (IEC, 2013) using data from a test site (Wagner et al., 2014). The test site consisted of a small 500 kW wind turbine with a hub height of 36 meter and a rotor diameter 41 meter. First the organizations were asked to calculate annual energy production given the wind speed data and the power curve. The wind speed data was preprocessed by the authors, such that the organizations could not apply different preprocessing methodologies, hence the authors could focus on differences in the rest of applied methodologies. Second, the organizations were asked to calculate the mean wind speed using the rotor equivalent wind speed method proposed in by the IEC committee draft. It was concluded that the shear was not so large for this test site so that the rotor equivalent wind speed method did not improve the power performance measures. Furthermore different interpretations of the standard yielded different estimated annual production figures, which had been resolved by finding consensus on the preferred method.

2.3   Power performance standard

The power performance measurements of wind turbines have been standardized by the IEC. The full name of the standard is "Wind turbines – Part 12-1: Power performance measurements of electricity producing wind turbines". The first edition is from 2005 and at the moment of writing this research there is a drafted second edition version. The second edition version enables measurements with remote sensing devices.

An overview of the different calculations between the two methods is shown in Figure 2.9. The different steps are explained shortly in this section, while a more detailed approach including formulas is provided in the Methodology section.
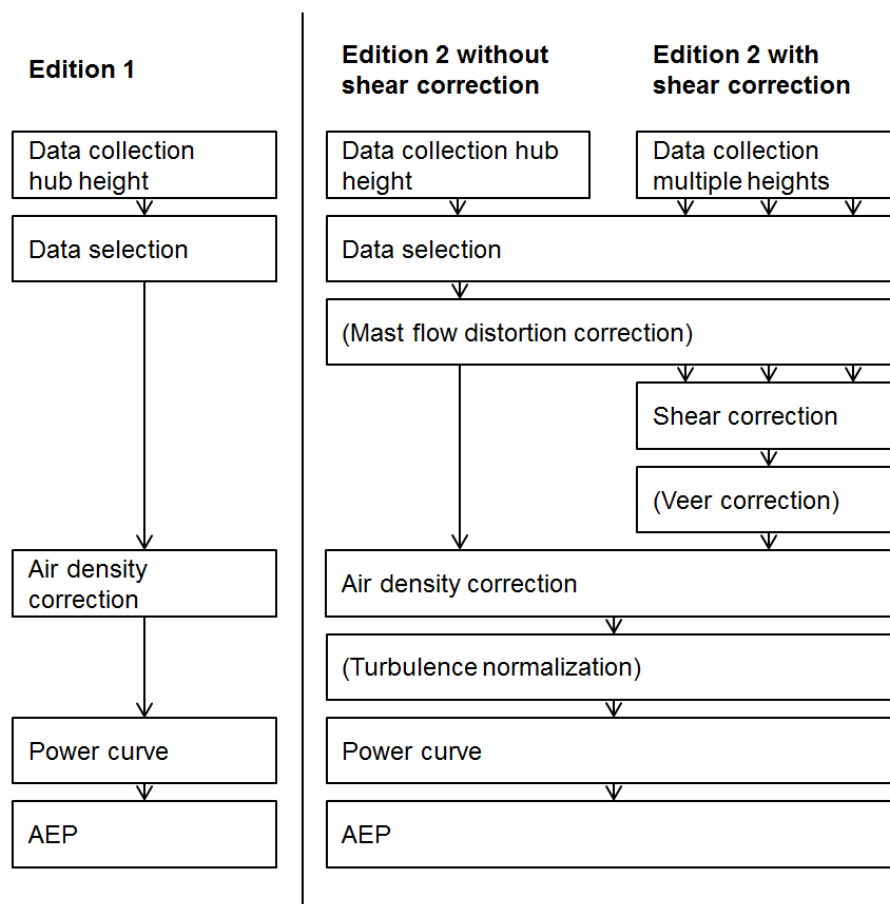
Figure 2.9: Comparisson of IEC 61400-12-1 Edition 1 and Edition 2. Optional steps are shown in brackets [()]. For edition 2 there are two possible data flows for the Edition 2 standard; starting with hub height measurements (represented with one arrow) or starting with measurements of multiple heights (represented with multiple arrows). The shear correction combines the wind speeds at multiple heights to one wind speed. Based on IEC (2005) and IEC (2015).

2.3.1   IEC 61400-12-1 Edition 1

Data collection consists of gathering 10-minute average data, including wind speed, wind direction and wind turbine status signals. Furthermore air temperature and air pressure are measured.

Data selection consists of rejecting all data out of valid measurement conditions. Excluded are the times where the wind comes from directions where it is disturbed by objects. Also moments where the turbine shows status errors are excluded.

Then the data is normalized. In Edition 1 only site calibration and air density correction are applied. Site calibration means to calculate the systematic differences between the measurements at the location of the meteorological mast and the measurements at hub height of the wind turbine. This can be done for example for complex terrains to account for the difference in height between the meteorological mast and the wind turbine. Site calibration can be performed by temporary positioning a second meteorological mast at the location where a turbine will be placed later. The second normalization of Edition 1, air density correction, enables comparison between te performance of wind turbines over periods or locations with different air density. Because the power in the wind is dependent on air density according to formula 2.5.

$$P = \frac{1}{2}\,\rho A U^3 \tag{2.5}$$

$$c_p = \frac{P}{\frac{1}{2}\,\rho A U^3} \tag{2.6}$$

Where
P is the power extracted from the wind;
ρ is the air density;
A is the swept rotor area;
U is the horizontal component of the wind speed.

The power curve is obtained by defining wind speed bins of 0.5 m/s wide. Within a bin, the wind speed and air density are averaged.

In order to find the AEP, the power curve (P,u)-curve is combined with the wind speed distribution function (u,t)-curve and the number of hours in a year. In this way one could translate the power curve to the energy yield for the wind regime at the site.

2.3.2   IEC 61400-12-1 Edition 2

For Edition 2, all steps of Edition 1 are applied, but extended with extra steps. Most steps are optional. However, the wind shear correction is obligatory when remote sensing devices are involved or when a meteorological mast is present that can measure above hub height, as shown in Table

Table 2.2: Measurements configurations and its typical applications in the IEC 61400-12-1 Edition 2 standard (IEC, 2015).

Configuration		Application		Normalization	
Met mast	Remote sensing	Wind turbines	Terrain	Air density	Shear
1. To hub	All heights	Large	Flat	x	x
2. Below hub	All heights	Large	Flat	x	x
3. Above hub		Large and small	All	x	x
4. To hub		Large and small	All	x	

2.2.

The first additional option of Edition 2 (Figure 2.9) is mast flow distortion. This is an optional measure to calculate what wind speed that would have been measured when the measurements would not have been affected by the meteorological mast its wake.

Wind shear correction means taking into account the variation of wind speed with height. At the ground the wind speed is 0 m/s and the wind speed increases with height. To capture the effect of the difference in wind speed with height, wind shear correction can be carried out. For example, an area-averaged wind speed could be calculated, which contains more information than only the wind speed at hub height.

Wind veer is the change of wind direction with height. Veer can be observed by comparing the wind vanes at different heights as displayed in Figure 2.10. Wind veer correction takes into consideration the varying wind direction with height. When there is a large wind veer, one can argue that the energy that could be captured within a rotor disc reduces. One way of seeing this is that the wind velocity vector is not perpendicular to the rotor disc on all heights, which reduces the possible energy that a rotor could extract. In this assumption the rotation of the blades are not taken into consideration (but could lead to interesting effects).

Figure 2.10: Wind veer. The foto is taken underneat the meteorological mast at the Princess Alexia site. The wind vanes are positioned at 46 and 96 meter above ground level.

Turbulence intensity normalization takes into account the variation of wind speed around the mean wind speed. Since only 10-minute wind speed averages are taken into account that information would be lost otherwise. With a certain wind speed, for example 8 m/s, the energy in the wind is higher when there was turbulence then when there was no turbulence because the energy in the wind increases with the third power of the wind speed (Equation 2.5).

Chapter 3

Methods

In the methods section, the measurement campaign will be described followed by the data processing methodology. Thereafter sections elaborate on methods for validating the Lidar, comparing power performance tests and Lidar outages and error checking.

3.1 Measurement campaign

A measurement campaign was held at the Princess Alexia wind park in municipality Zeewolde, province Flevoland, the Netherlands. The site consists of 36 wind turbines with a rated power of 3.37 MW and a hub height of 80 meter. This site is characterized by flat terrain with open farmland. The open farmland is partly overgrown with small trees and some farm houses are situated within the site. The site is surrounded by turbines to the North and West, and the site is surrounded by forest to the East and West (Figure 3.1).

This site offers the opportunity to do IEC compliant power performance measurements because the site is equipped with one meteorological mast which is located next to two wind turbines . A Lidar was positioned next to the meteorological mast to enable a comparison. The positions of the Lidar and meteorological mast is shown in Figure 3.1 and is elaborated on in Section 3.1.2 and Section 3.1.3.

The measurement heights for the Lidar and meteorological mast are illustrated in Figure 3.2. The wind speed measurements of the Lidar and meteorological mast are at the same height. The same holds approximately for the wind direction (within 2 meter height difference, which is considered negligible).

The measurement campaign started on September 25, 2015, when the Lidar was available and there was time available for installing the Lidar. The measurement campaign lasted until January 2, 2016, because data of the meteorological mast was available until then. The Lidar was repositioned to an other location on February 13, 2016 because data collection for the power performance test was completed (Section 3.5.1) and time was available for repositioning the Lidar.
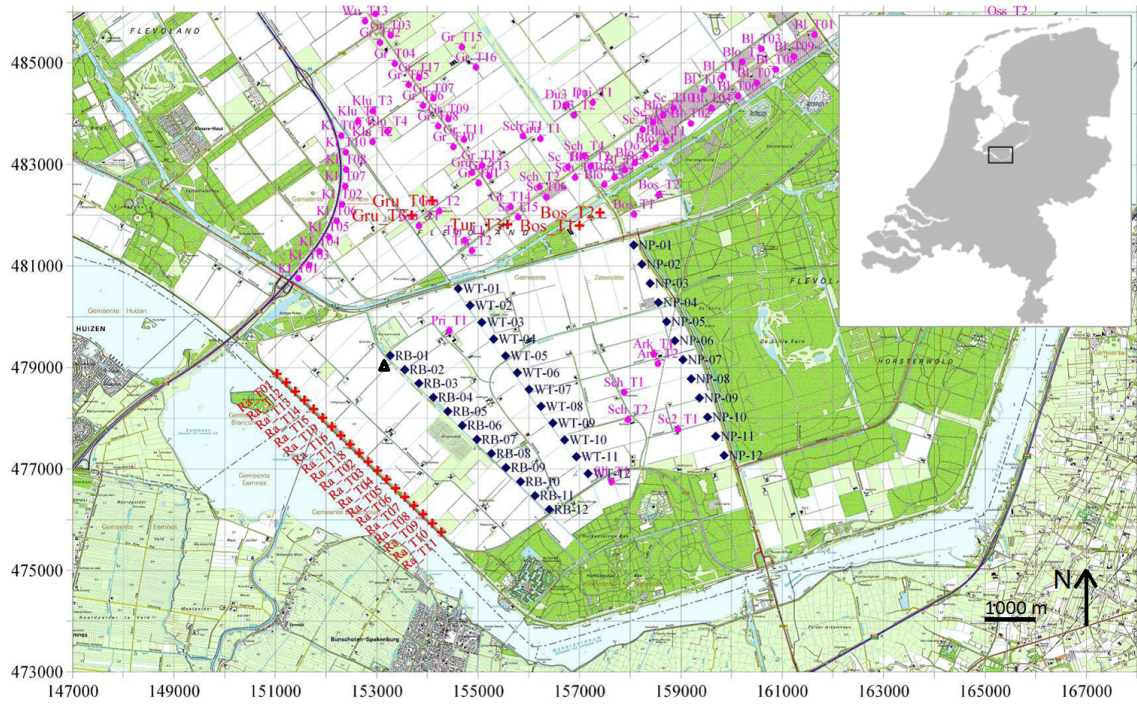
Figure 3.1: Site layout (Garrard Hassan, 2010) with inserted map of the Netherlands. The x and y axis are in meters. Blue diamonts indicate turbines of the Princess Alexia site. Red plusses and purple dots present turbines of other sites. The black triangle is inserted to represent the meteorological mast and lidar.
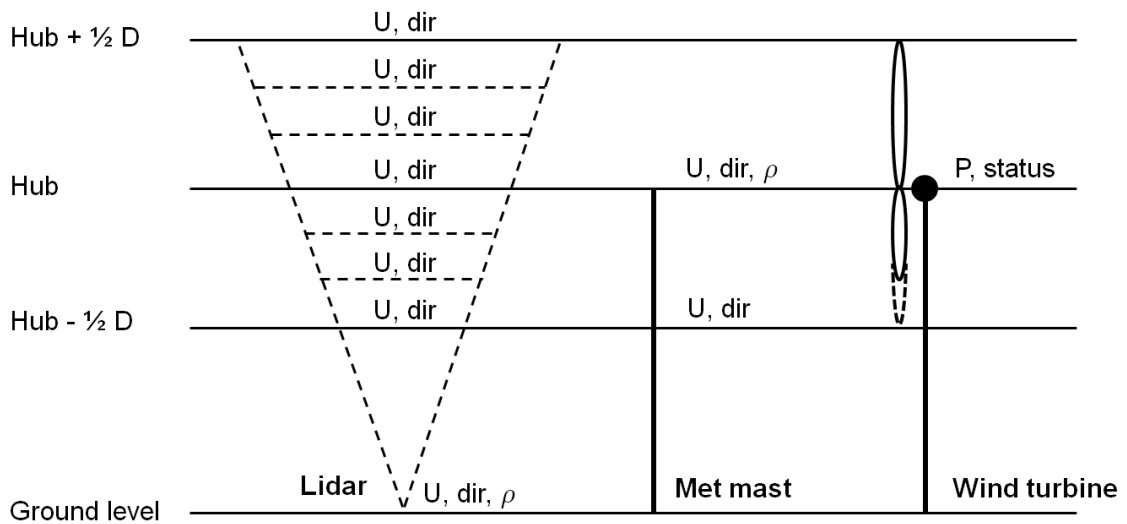
Figure 3.2: Schematic measurement setup, wind speed (u), wind direction (dir), power (P) and turbine status signal (status). Air density (ρ) is measured using temperature, pressure and humidity measurements.
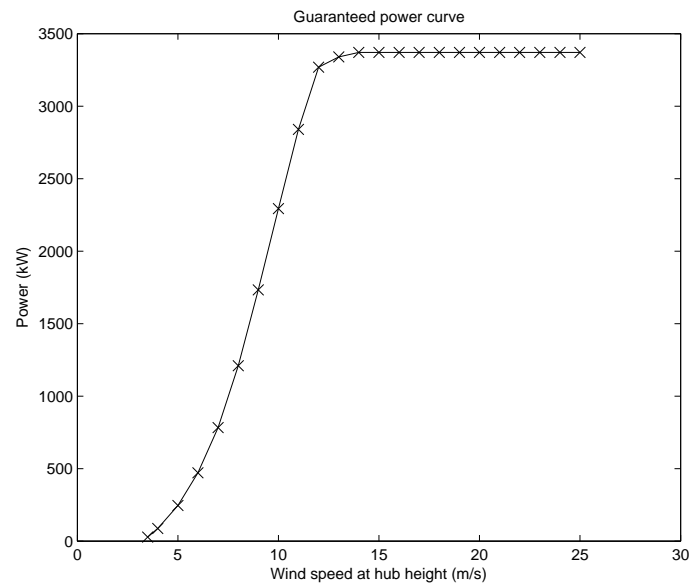
Figure 3.3: Guaranteed power curve.

3.1.1 Wind turbines

All Princess Alexia wind turbines are Senvion 3.4M104 wind turbines with 3.37 MW rated power, 98 meter hub height and 104 meter rotor diameter (Table 3.1). The guaranteed power curve for these wind turbines is shown in Figure 3.3. The guaranteed power curve holds for inner envelope conditions summarized in Table 3.2. Other specifications of the power guaranteed are kept confidential. As stated in Table 3.2, the contract states that wind speed measurements should be done with a Thies First Class anemometer. Thies is a brand and First Class is the product name. The product name refers to class 1 certification which means that the for a 10 m/s actual wind speed, the difference between the measured wind speed and actual wind speed is < 1 m/s. When the wind speed is lower than 10 m/s the deviation is allowed to be larger and for higher wind speeds the uncertainty must be lower. The certification procedures can be found in IEC 61400-12-1 Edition 1 and 2, Annex I and J (IEC, 2005, 2015).

Table 3.1: Wind turbine specification (WICO, 2015).

Parameter	Value
Manufacturer, type name	Senvion SE, 3.4M104
Rated power	3370 kW
Wind speed rated, cut in, cut out	13.5 m/s, 3.5 m/s, 25 m/s
Hub height	98.0 m
Rotor diameter, swept area	104 m, 8495 m^2

Table 3.2: Inner-envelope conditions for the guaranteed power curve of wind turbines at Princess Alexia wind farm.

Parameter	Value
turbulence intensity	$6\% \leq TI < 12\%$
shear exponent lower tip to hub height	≤ 0.2
air density at location	$\geq 1.13 kg/m^3$
temperature	$\leq 35^o C$
power factor	$\cos(\phi) \approx 1$
wind speed measurement	with a Thies First Class anemometer
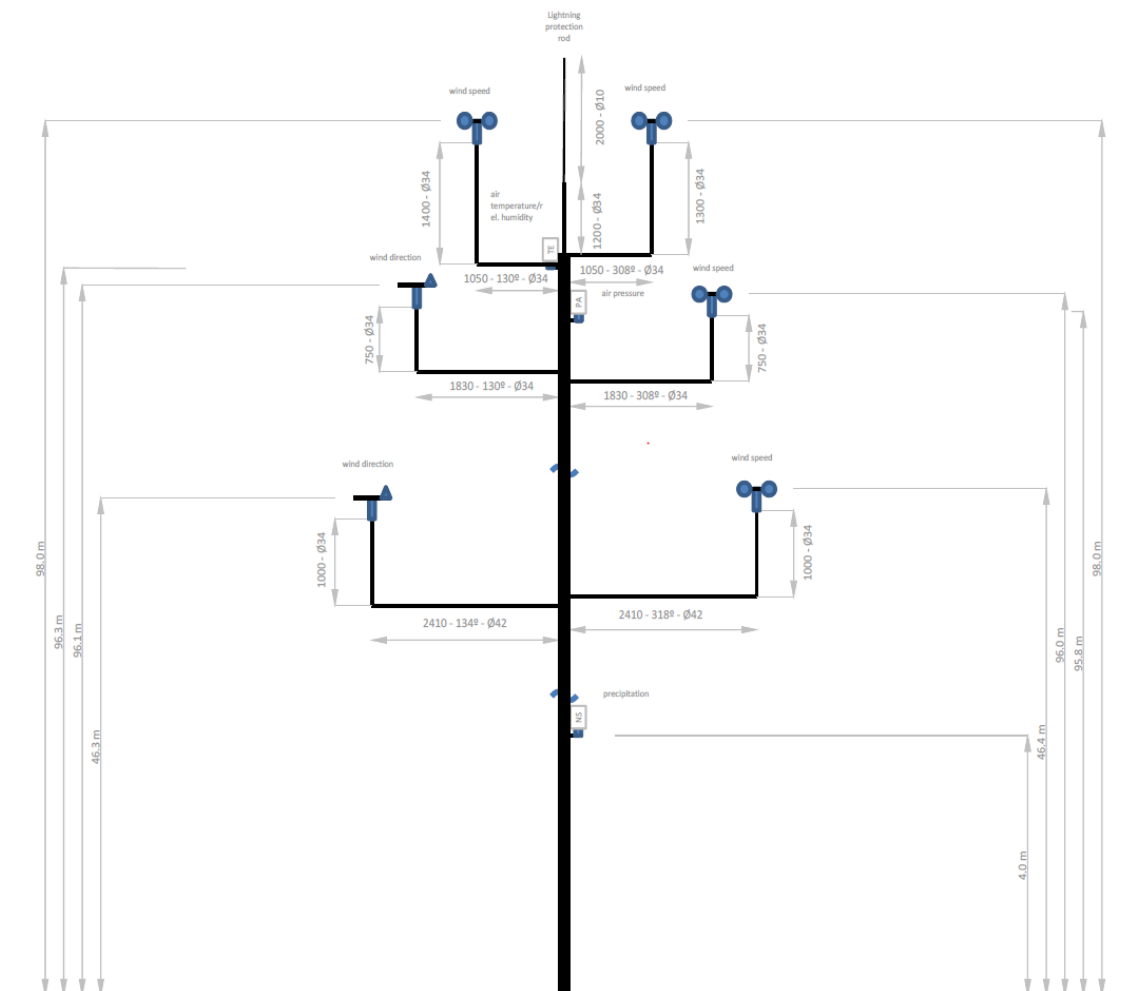
Figure 3.4: Meteorological mast (WICO, 2015). Schematic overview, not on scale.

3.1.2 Meteorological mast

The Princess Alexia wind farm is equipped with a 98 meter meteorological mast which is positioned next to the two most North-East situated wind turbines E01 and E02. The distance between the meteorological mast and the two turbines is between 2 and 4 rotor diameters which is compliant with the IEC 2005 and proposed 2015 standard (IEC, 2005, 2015). The meteorological

mast setup is shown in Figure 3.4. The sensors at the meteorological mast are described in Table 3.5 which include wind speed measurements at hub height using 2 sensors and wind speed measurement measurement at hub height minus half a rotor diameter. This meteorological mast is compliant for IEC power performance measurements (WICO, 2015), due to the height, location, and sensors.

3.1.3   Lidar

A ZephIR 300 Lidar was newly bought by Nuon/Vattenfall and installed at the site on September 24, 2015 by the energy consultancy company Ecofys. The specifications of the Lidar are shown in Table 3.3 and a picture of the Lidar is shown in Figure 2.4. The cone angle of 30 degrees is equal to an elevation angle of 60 degrees.

Table 3.3: Lidar specifications (ZephIR, 2015c).

Parameter	Value
Type	Continuous wave coherent doppler (Section 2.1.2.)
Manufacturer	ZephIR Ltd.
Type name	ZephIR 300
Version name	DM, dual mode, can also be installed at a nacelle
Beam orientation, half cone angle	Upward looking, 30 degrees

The Lidar was installed on the ground next to the existing meteorological mast so that measurements could be compared. The position was selected with guidance from the ZephIR 300 Deployment Guide, chapter "Siting Adjacent to a Met Mast", in order to obtain the best possible measurements (ZephIR, 2015b). A position close to the mast has the advantage that the beams do not illuminate any moving parts at the meteorological mast such as its anemometers. Also, such a position minimizes measuring wake effects of the meteorological mast, because the beam quickly moves away with height due to the 30 degree cone angle. The Lidar was positioned to the South-East of the meteorological mast where the meteorological mast would not obscure upwind or downwind measurements in the prevailing wind direction from South-West, as well as having a limited number of guy wires obscuring the measurement window. The Lidar position is shown in Figure 3.5.

We defined the Lidar measurement heights for wind speed and wind direction which were configured by Ecofys. We selected the measurement heights to compare Lidar the measurements with the meteorological mast, to perform power curve verification with a hub height approach and similarly for a rotor equivalent wind speed approach. The heights as chosen for the rotor equivalent wind speed are explained in Section 3.5.3. Other heights were chosen for reasons outside the scope of this study The chosen heights are shown in Table 3.4.
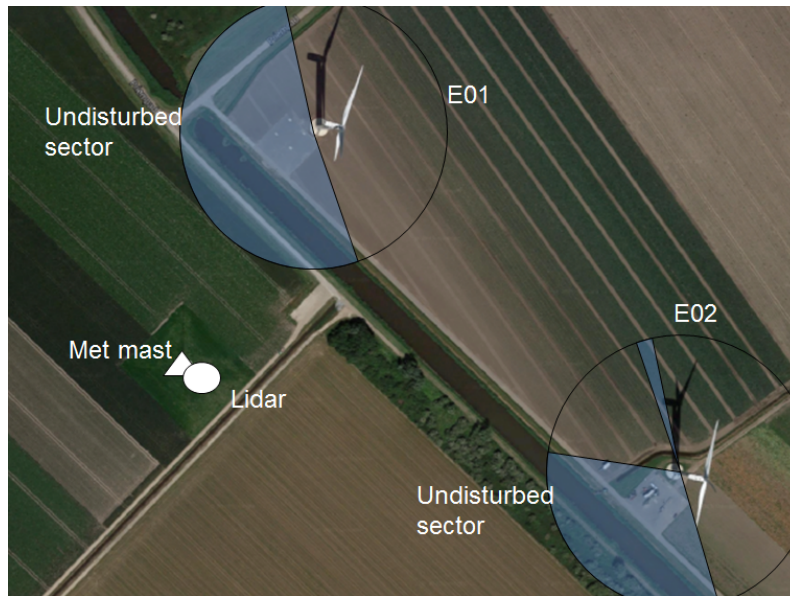
Figure 3.5: Location of meteorological mast, Lidar and wind turbines (Google Maps, 2015)

Table 3.4: Choosen lidar measurement heights for wind speed and wind direction.

Nr.	Height (m.a.g.l.)	Met mast height	REWS height	Turbine height
1	9			
2	37			
3	46.3	y		Lower tip (approx)
4	56.4		y	
5	77.2		y	
6	98	y	y	Hub
7	118.8		y	
8	139.6		y	
9	150			Upper tip
10	175			
11	200			

Besides the wind measurements, the ZephIR 300 measures air pressure, air density and temperature with a little meteorological station that is mounted on the ZephIR 300, giving measurements at 1 meter above ground level (Table 3.5). The meteorological station was shown on the top left of the lidar in Figure 2.4.

Table 3.5: Measurements of meteorological conditions its measurement heights in meter above ground level.

Variable	Measurement	Meteorological mast	Lidar
Wind speed	Wind speed	46.4, 96.0, 98.0 (2x)	Multiple (see Table3.4)
Wind direction	Wind direction	46.3, 96.1	Multiple (see Table3.4)
Air density	Air pressure	95.8	1
	Temperature	96.3	1
	Relative humidity	96.3	1

3.2   Data flow and data pre-processing

Matlab code was written to perform the calculation for which the general data flow is described in Figure 3.6. For each research question the data filtering and and calculations can be adjusted.
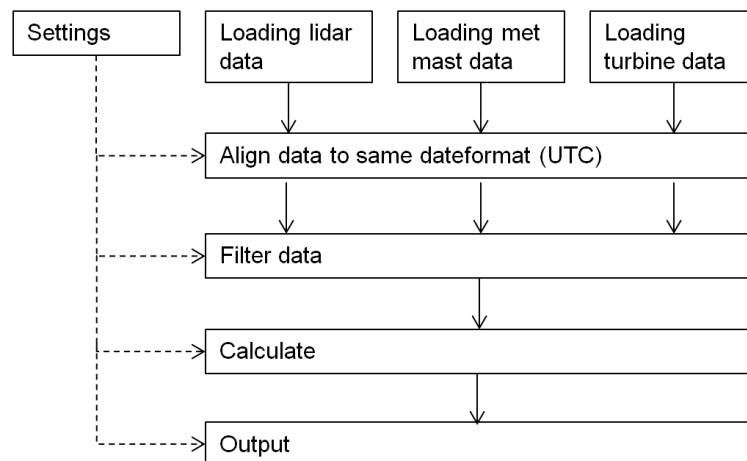
Figure 3.6: Data flow.

Data collection for meteorological conditions was performed using the meteorological mast and the lidar as was shown in Table 3.5. Data from the meteorological mast SCADA system is obtained via a Wind Consult, who sent the data in Comma Separated Value files.

Lidar data was obtained via Ecofys. The lidar has a modem that sent the data to Ecofys who uploaded it directly to a server of Nuon/Vattenfall. This data then was processed by the ZephIR data interpretation software by colleague Jim Hough, who uploaded the processed data to a shared folder of the Wind&Site team. The data processing with the ZephIR software comprised of standardized steps. Errors were recorded in the data file with an error code. For example in the wind speed data, the wind speed was recorded as 9998 or 9999 when there was an error. Therefore every 9998 and 9999 was replaced by a missing value, and recorded in a separate "Error 9998 flag" or "Error 9999 flag" variable.

Data from the wind turbine was obtained in two ways. Data was obtained directly from the Supervisory Control And Data Acquisition (SCADA) system of the wind farm itself which can be

Table 3.6: Time zone specifications of each data input file.

Data	Timezone	Description
Lidar CSV files	UTC	Stated as "Time sync: UTC +0 hrs"
Metmast xls file	UTC+1	Stated as "Einheit: MEZ". Mitteleuropäische Zeit which is Central European Time
Turbine data	UTC	Stated as "UTC Timestamp". Obtained using the Wind Data Analyzer software

accessed via the internal software called Vattenfall Wind Power Data Center. Additionally for wind turbines E01 and E02, some data was logged with sensors installed by Wind Consult too. These measurements were power and status signals. These measurements were done with IEC 61400-12-1 Edition 1 calibrated equipment (WICO, 2015).

Data was converted from its own time zone to a common timezone and only data was kept where all data sources contain measurements. Time alignment was performed by calculating the Coordinated Universal Time (UTC) time for each data source based on its timezone shown in Table 3.6. Furthermore the meteorological mast data was recorded at the middle of the 10 minute interval in stead of in the beginning of the 10 minute interval as with the other sources. Therefore on top of the conversion from timezone, 5 minutes were subtracted from the meteorological mast time stamps to synchronize with the other sources.

It was checked whether the data sources were aligned in time properly, of which an example is shown in Figure 3.7. The meteorological mast and Lidar indeed show the same pattern of wind speed measurement over time (Figure 3.7a). The meteorological mast and wind turbine E01 also shown a synchronized pattern. The power output of the wind turbine was logged by equipment of Wind Consult that was synchronized with the meteorological mast data. Slight differences in power output could be observed. This is due to the different location in the electrical circuit at which the voltage is measured in the wind turbine.

(a) Lidar with meteorological mast

(b) Meteorological mast with Wind Turbine E01
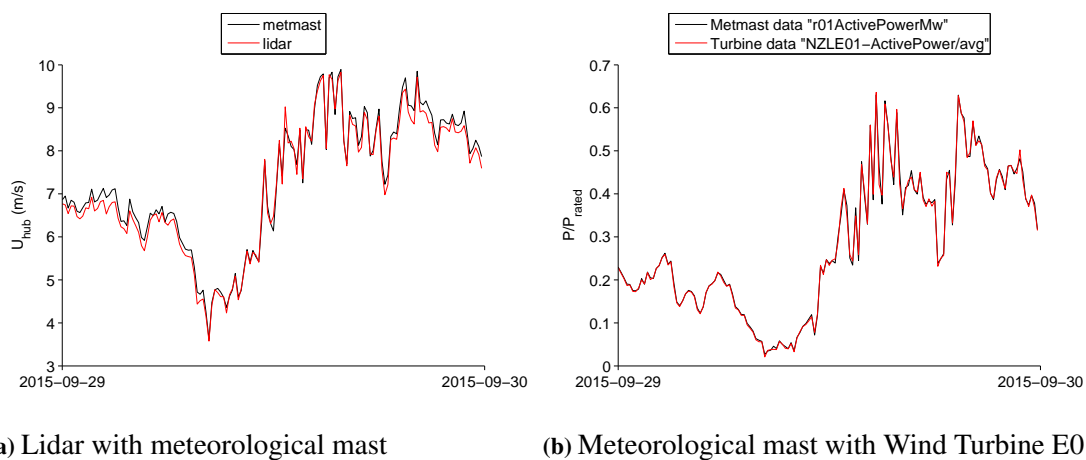
Figure 3.7: Data source time synchronzation check.

3.2.1 Meteorological mast wind speed

Since the Lidar was validated against the meteorological mast it is important to choose which data is used from the meteorological mast. Starting with the wind speed. There are two anemometers which are positioned at the meteorological mast with an angle on the horizontal plane of 130 and 308 degrees from the North as shown in Figure 3.8. When the wind blows from one direction, the sensor behind the meteorological mast is in the wake of the mast and therefore not measuring the true wind speed. The readings from the two anemometers were plotted against time including its difference. Also to visualize the effect of the wind direction, the difference was plotted against the wind direction.

The difference in wind speed readings from the two anemometers at 98 meter above ground level at the meteorological mast is shown in Figure 3.9. The readings from the two anemometers look similar in the upper plot. The difference however can be significant, as shown in the lower plot. When plotting the difference against the wind direction in Figure 3.10, it is clearly seen that the difference in wind speed reading is caused by the flow distortion of the meteorological mast. The wind speed therefore is taken from the sensor closest to direction where the wind is coming from. The angles between the boom angles are 39 and 219 degrees. Therefore, when the $39 \leq$ direction < 219, the measurements are taken from sensor A2 and otherwise from sensor A1.
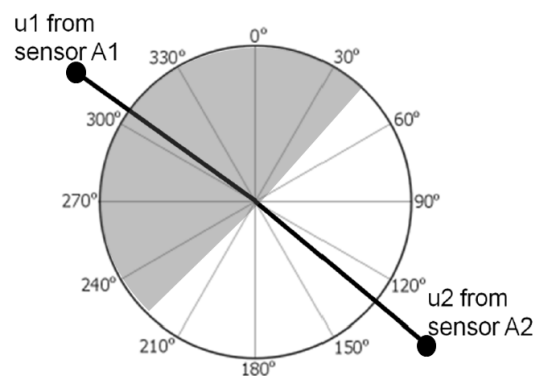
Figure 3.8: Boom angles of the hubheight windspeed sensors at the meteorological mast (seen from the top).
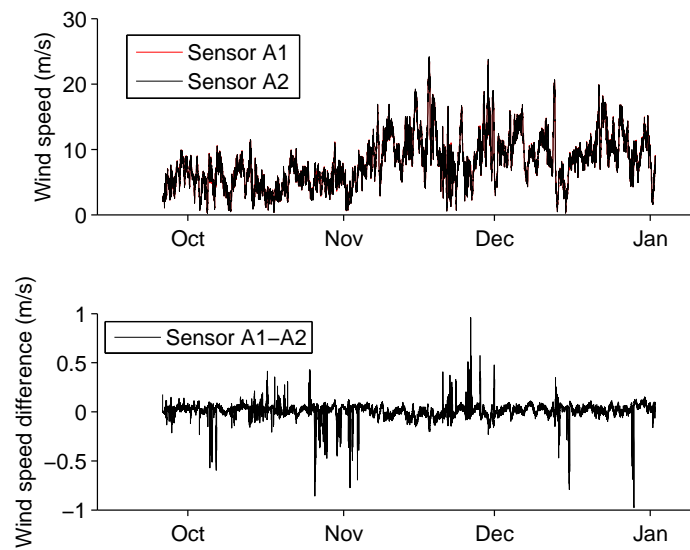
Figure 3.9: Difference in anemometer readings of the meteorological mast at hub height.
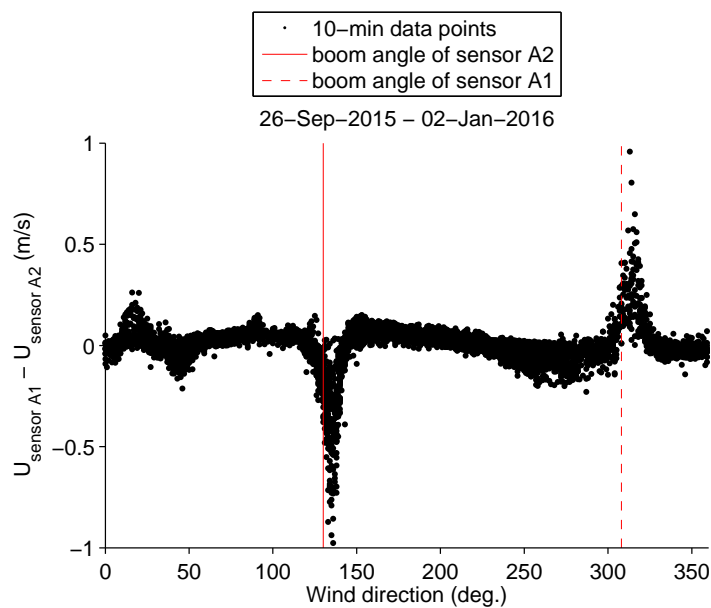
Figure 3.10: Difference in anemometer readings with wind direction.

3.3 Meteorological conditions at the site

Many wind studies start with summarizing the meteorological conditions at the site during the measurement campaign. In this way a general feeling for the conditions is shown, it gives insights needed for some analysis and it allows for comparison between multiple studies. Furthermore

these figures can be of use for evaluations within the report.

All graphs were shown based on input from the meteorological mast, because the lidar was not validated at this point, and to make the figures comparable with other reports that base these figures mostly on meteorological mast inputs. The wind direction for the from the wind vane 2 meter below hub height and cup anemometers at hub height, which has a negligible difference in wind direction with wind vane that would be installed at hub height.

Meteorological conditions were shown using a wind rose to show which wind speeds occur from which wind direction sector.

Furthermore a wind speed distribution was shown. The wind speed distribution function was estimated. This could be used later to calculate the annual energy production figures. The Weibull parameters were estimated using the method of Justus in Equation 3.2. This is a good estimate when in Equation 3.1 $1 \leq k < 10$ (Manwell et al., 2010) (Justus, 1978), which was the case during this measurement campaign.

$$ k \;=\; \left(\frac{std(u_{10min})}{mean(u_{10min})} \right)^{-1.086} \tag{3.1} $$

$$ A \;=\; \frac{mean(u_{10min})}{\Gamma(1 + 1/k)} \tag{3.2} $$

Where Γ is the gamma function that interpolates numbers n in the factorial function $f(n) = n!$. The gamma function was implemented using the build-in Matlab function Gamma.

3.4   Lidar measurement validation

Since the Lidar was positioned next to the meteorological mast, the Lidar could be validated. When a short meteorological mast is accompanying a Lidar for power performance test as proposed in the IEC 61400-12-1 Edition 2 standard, then for the Lidar only wind speed measurements are needed. However, when the Lidar would be used to measure the power performance of a turbine where no meteorological mast is present, then it is also of importance to measure other parameters. These parameters are wind direction, air density (using temperature, pressure and humidity) and possibly turbulence intensity (for filtering certain conditions that are within the power performance guarantee of the wind turbine).

Time series plots were made, showing both the Lidar measurements and meteorological mast measurements over time, to get an easy-to-interpret overview of the differences and whether these were bound to specific periods. A linear regression was performed to show a more detailed relation between the meteorological mast and Lidar measurements.

For the power performance test, only wind speeds above cut-in wind speed are needed for evaluation. Also the wind speed, wind direction and turbulence intensity were more difficult to measure for the Lidar during the lower wind speed. For these variables we zoomed in to the occurrences

where the wind speed was higher than the cut-in wind speed. For the variables where the wind speed is not of influence, e.g. for the air density variables, the analysis was performed over the whole data set in order to be better able to generalize over the results.

The wind speed here was taken from the Lidar, as the data selection from the Lidar would be used for data filtering when a Lidar is used for a power performance test.

3.4.1 Wind speed

Additional criteria were tested for the wind speed. The Lidar wind speed validation was based on the Norsewind criteria as shown in Table 3.7. Basically the linear regression on the wind speed measurements is divided in multiple wind speed segments and for each segments the criteria are tested. The Norsewind criteria were chosen because these are supported and evaluated by a broad range of parties. The validation was done for 46 and 98 meter above ground level where meteorological mast and Lidar measurements coincide. The amount of data valid data points required here was set on 500, which is not of any influence for this data set. Whichever realistic requirement would be set, that requirement would have been met.

An adjustment was made to the original Norsewind criteria. The 4 m/s wind speed minimum was changed into 3.5 m/s, because that is the cut-in wind speed of these wind turbines and therefor important to measure well.

Table 3.7: Norsewind criteria adopted from Hasager et al. (2013).

Parameter	Criteria	Ranges (Height and Speed)
Absolute error	<0.5 m·s^{-1} for $2 < u < 16$ m·s^{-1} Within 5% above 16 m·s^{-1} Not more than 10% of data to exceed those values	All valid data
Data availability	Assessed case by case Environmental conditions dependency	All valid data
Linear regression Slope	Slope between 0.98 and 1.01 <0.015 variation in slope between u-ranges (b) and (c)	Heights from 60 to 116 m u-ranges: (a) 4–16 m·s^{-1}, (b) 4–8 m·s^{-1}, (c) 8–12 m·s^{-1}
Linear regression Correlation coefficient (R^2)	>0.98	Heights from 60 to 116m u-ranges: (a) 4–16 m·s^{-1}, (b) 4–8 m·s^{-1}, (c) 8–12 m·s^{-1}

3.4.2 Air density

The air density can be calculated based on air temperature, air pressure and with or without considering the relative humidity. The difference between including and excluding relative humidity is fairly small. For the Lidar measurement validation, the relative humidity was used in the calcu-

lations.

$$\rho_{10min} \quad = \quad \frac{1}{T_{10min}}\left(\frac{B_{10min}}{R_0} - \phi * P_w\left(\frac{1}{R_0} - \frac{1}{R_w}\right)\right) \tag{3.3}$$

$$P_w \quad = \quad 2.05 * 10^{-5} * e^{0.0631846*T} \tag{3.4}$$

Where

ρ_{10min} is the measured air density;

T_{10min} is the measured air temperature;

B_{10min} is the measured air pressure;

R_0 is the gas constant for dry air ($287.05 \ Jkg^{-1}K^{-1}$);

ϕ is the relative humidity;

P_w is the vapor pressure;

R_w is the gas constant of water vapor ($461.5 Jkg^{-1}K^{-1}$).

Measurements were not performed on the same heights, because the Lidar measures it by the meteorological station mounted on the Lidar. For the power performance test, the measurements are to be corrected to hub height. Therefore the measurements of temperature and air pressure are corrected to 98 meter above ground level.

The air temperature is corrected to hub height using the constant gradient of temperature (ISO, 1975).

$$T = T_{base} + L * (H - H_{base}) \tag{3.5}$$

Where

T is the air temperature at hub height;

T_{base} is the air temperature at ground level;

L is the constant temperature gradient -0.0065 K/m (ISO, 1975);

H is the hub height;

H_{base} is ground level height.

Air pressure can be corrected using formula 3.6 (Thøgersen, 2005).

$$P = P_b * \left(\frac{T_{base}}{T_{base} + L * (H - H_{base})}\right)^{-\frac{g_0 * M}{R * L}} \tag{3.6}$$

Where

P is the pressure at hub height;

P_{base} is the pressure at ground level;

g_0 is the gravitational constant at sea level;

M is the average molar mass of air, 0.02897 kg/mol;

R is the gas constant 287.05 J/(kg K).

The relative humidity was not corrected for height, because its influence on the air density is very small, and this correction is not suggested in the Edition 2 standard (IEC, 2015).

3.4.3 Wind direction

As it was found that the wind direction measurement of the Lidar was off by 180 degrees for some periods, extra analysis were performed to check how this could be resolved. The wind direction measurements of the meteorological station at the Lidar and wind direction measurements at the wind turbine E01 were compared to the meteorological mast measurements to find whether the wind direction measurements could be corrected.

3.4.4 Turbulence intensity

Turbulence intensity was a output from the Lidar directly. For the meteorological mast, the turbulence intensity was calculated. Turbulence intensity is defined as:

$$TI = \frac{\sigma_{u10}}{\overline{U_{10}}} \qquad (3.7)$$

Where

$\overline{U_{10}}$ is the 10-minute mean wind speed;

σ_{u10} is the standard deviation of the 10-minute wind speed.

The lidar outputs the turbulence intensity as number and the meteorological mast outputs the mean wind speed and its standard deviation.

3.5 Power performance tests

For multiple research questions, the power performance test was of importance. Here, the methodology for a power performance test is explained, where-after the different settings are explained that were used to answer the different sub-questions. The methodology is explained per step of the power performance test. First the steps needed for the IEC Edition 1 power performance test are explained. Thereafter the additional steps for Edition 2 are explained (the steps were shown for the different editions in Section 2.3, Figure 2.9).

3.5.1   Meteorological mast and Lidar at hub height

Data selection

Data filtering is the same for the current as the proposed version (IEC, 2005, 2015). Data selection for power curve calculation is based on wind directions, atmospheric conditions and turbine operation. Data was excluded was based on criteria from the IEC power performance standards as quoted (IEC, 2005, 2015) and site specific criteria for the next categories.

a) "External conditions other than wind speed are out of the operating range of the wind turbine". There were two methods for selection. When te standard IEC power curve was tested, no conditions were applied as being outside the operating range of the wind turbine. When the guaranteed power curve was tested. Data was filtered to match the contracted inner-envelope conditions (Table 3.2). Turbulence intensity was explained in Equation Equation 3.8. The shear exponent is defined as:

$$\alpha_{10min} = \frac{\log(U_{10min,h2}/U_{10min,h1})}{\log(h2/h1)} \tag{3.8}$$

Where
α_{10min} is the shear exponent;
$h2$ is the upper height;
$h1$ is the lower height.

b) "The wind turbine cannot operate because of a wind turbine fault condition". The turbine is considered in operation when the parameter $faultLossTurbineAvg$ is equal to zero.

c) "The wind turbine is manually shut down or in a test or maintenance operating mode". The same condtions were used as for b.

d) "Failure or degradation (e.g. due to icing) of test equipment". Only periods with temperatures > 2 degree Celsius were included.

e) "Wind direction outside the measurement sector(s)".There are no changes for the measurement sector criteria of the current and the proposed IEC power performance standard (IEC, 2005, 2015). Therefore the same measurement sector was included as done by Wind Consult for a power performance test in February and March 2015 (WICO, 2015), who found the wind direction sectors in compliance with the IEC Edition 1 standard. For wind turbine E01 and wind turbine E02 the undisturbed sector was calculated using IEC 61400-12-1 Edition 1 Annex A by Wind Consult (WICO, 2015). The undisturbed flow for the tested wind turbine E01 is 163 to 348 degrees respectively to the compass rose based on the obstacles in and around the wind farm by WIND Consult (WICO, 2015). For turbine E02 the undisturbed sector is between 164 and 281 degrees and 343 and 348 degrees (Figure 3.11 and Figure 3.12).

f) "Wind directions outside valid (complete) site calibration sectors". No site calibration was

performed before building the wind turbines, because there is no complex terrain (site cal-
ibration was explained in Section 2.3.1). It is assumed that for the undisturbed flow, the
wind speed measurements at the meteorological mast are not significantly different from
the measurement when a meteorological mast would have been placed at the location of the
wind turbine.

g) Hysteresis loops in the cut-out algorithm were to be excluded from the power performance
check (IEC, 2005, 2015). A hysteris loop means that the turbine is shut down due to wind
speeds higher than cut-out wind speed but does not restart directly when the wind speed
reaches a lower than cut-out wind speed. Hysteris loops were checked for by plotting power
and wind speed for the the 24 hours after wind speed has reached cut out wind speed minus
2 m/s. Periods were excluded when the power was significantly smaller than what would be
expected according to the power curve.

- For wind turbine E01 data was excluded from November 18, 2015 00:50:00 UTC until
  and excluding November 18, 2015 02:10:00 UTC and November 29, 2015 19:20 UTC
  (shown in Figure D.1).

- For wind turbine E02 November 18, 2015 00:40:00 UTC until and excluding Novem-
  ber 18, 2015 01:10:00 was removed, as well as November 2015, 18:40, 18:50 and
  19:20 UTC (shown in Figure D.2).

The ratio of included data was calculated for each filter individually. As well, the total ratio was
calculated.

Data normalization

After filtering, the data was used to calculate the power curve. Air temperature and air pressure
were corrected to hub height using Equation 3.5 and Equation 3.6. Air density was calculated using
Equation 3.4. For the Edition 1 standard, the relative humidity (ϕ) was not taken into account, so
that ϕ is set to zero. While for the Edition 2 standard, the relative humidity was taken into account.
Air density is calculated with Equation 3.3 in Section 3.4.2. The normalized wind speed then is
calculated as:

$$u_{normalized} \quad = \quad u_{10min} * \left(\frac{\rho_{10min}}{\rho_0} \right)^{1/3} \tag{3.9}$$

Where
u_{10min} is the measured horizontal wind speed;
ρ_0 is the reference air density $1.225 \, kg/m^3$ (IEC, 2005, 2015).
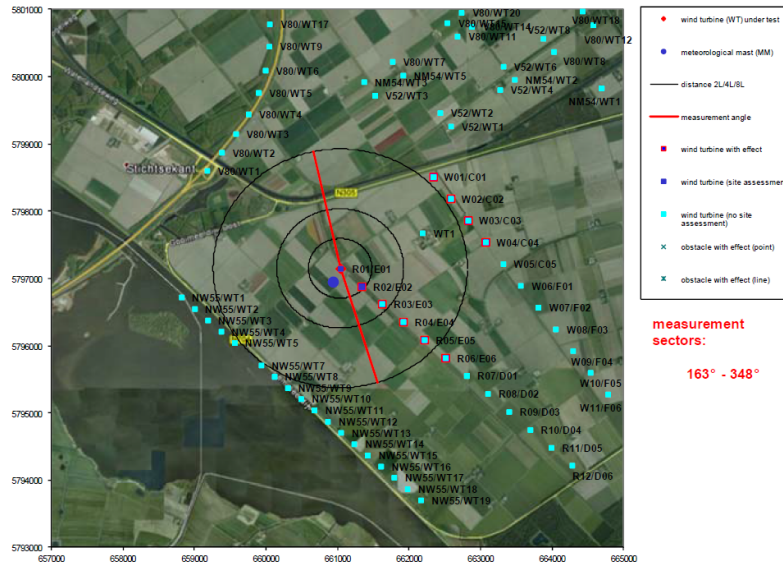
Figure 3.11: Undisturbed sector of wind turbine E01, 163 ≤ direction < 348 degrees resepectively to the compass rose as evaluated by WIND Consult (WICO, 2015)

.
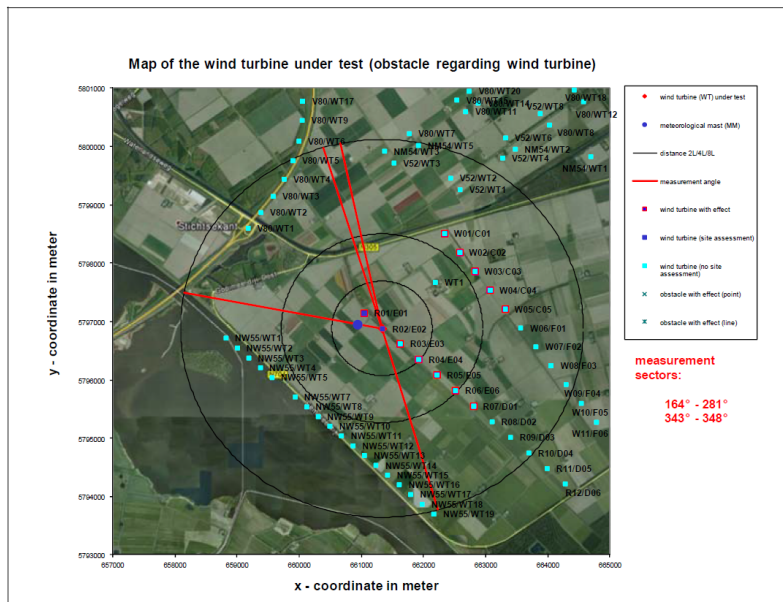
Figure 3.12: Measurement sector of wind turbine E02, 164 ≤ direction < 281 and 343 ≤ direction < 348 degrees resepectively to the compass rose as evaluated by WIND Consult (WICO, 2015)

.

Power curve

The data was binned to obtain a power curve.

$$P_i \quad = \quad \frac{1}{N_i} \sum_{j=1}^{N_i} P_{n,i} \tag{3.10}$$

$$U_i \quad = \quad \frac{1}{N_i} \sum_{j=1}^{N_i} U_{n,i} \tag{3.11}$$

Where
U_i is the normalized average wind speed in bin i. For example 3.75 m/s $<=$ u $<$ 4.25 m/s;
P_i is the average power output in bin i.

Data with the different devices is collected for which a minimum amount of data is needed. Data collection for the lidar started at September 24, 2015. The data collection needed to continue at least until each bin from cut-in wind speed minus 1 m/s to 1.5 times the wind speed at 85% of the rated power was filled with at least 3 10-minute data points, following both the Edition 1 the proposed Edition 2 IEC 2015 standard (IEC, 2005, 2015). With the exception that 1 bin was allowed to be missing. The bin for cut-in wind speed minus 1 m/s is 2.25 - 2.75 m/s. The upper wind speed consists of 16.25 - 16.75 m/s as calculated from the guaranteed power curve (Section 3.1.1). These criteria were met .

Incomplete power curves yield difficulties for calculating the estimated AEP. The IEC proposes to use a "measured" power curve or an "extrapolated" power curve. The measured power curve includes all data. In contrast, the extrapolated power curve only includes wind speed - power pairs up to the latest measured complete wind speed bin. The extrapolated power curve substitutes all power values higher than the latest complete bin above rated wind speed with rated power. Also it is allowed that to miss one bin between cut-in and rated wind speed which then is interpolated; this was not needed in this study. The number of needed completed bins normally is 3. For this study, a requirement of only 3 data points per bin was not stringent enough because the power curve far above rated wind speed (20-25 m/s) sometimes contained just enough data points including one occasion with low power (e.g. 1 MW). Then the comparison for AEP became greatly influenced by the one bad data point, which was not the purpose to find with these comparisons. Therefor, for this study it was chosen to set the minimum required bins to 15. The extrapolated power curve consists of all measured values and for incomplete wind speed bins, the power is estimated using linear interpolation from the latest complete data point up to rated wind speed and rated power.

AEP

The annual energy production was calculated by multiplying the yearly duration of each wind speed with the power output of that wind speed, hence, with the power curve (P,u).

$$AEP = N_h \sum_{i=1}^{N} [F(V_i) - F(V_{i-1})] \frac{P_{i-1} + Pi}{2} \qquad (3.12)$$

Where
AEP is the annual energy production; N_h is the number of hours in one year ≈ 8760;
N is the number of bins;
$F(V)$ is the cumulative probability distribution function for wind speed.

The probability distribution function for the wind speed is proposed as Weibull function in Equation 3.13. The IEC Edition 1 standard suggests to use a shape factor of 2, which yields a special case of the Weibull function, the Rayleigh function. While the IEC Edition 2 standard suggests to adjust the shape factor when enough is known about the wind conditions at the site (IEC, 2015).

$$F(V) = 1 - e^{\left(-\frac{V}{A}\right)^k} \qquad (3.13)$$

Where
V is the yearly mean wind speed;
A is the Weibull scale factor;
k is the Weibull shape factor.

The Annual Energy Production estimation in this study was used for comparing the impact of different methodologies. In this study, the Weibull shape factor of 2 was chosen, which is equal to a Rayleigh function. This value was chosen because they were used in earlier studies by Nuon/-Vattenfall and it was confirmed that the observed wind speed distribution during this measurement showed a good fit (As shown in Section 4 Figure 4.1).

Comparisson between power performance tests

The outcomes of the power performance test could be compared directly for outputs of the power performance calculations, for example the AEP or power curve plots, etcetera.

Furthermore the scatter in the power curve could be checked. When the rotor equivalent wind speed method would give a better understanding of the power in the wind, it would be expected that some of the the power - wind speed data points in the power curve would shift to a better wind speed bin. With the assumption that the wind turbine is performing similarly over time during the measurement period, it would be expected that the scatter would reduce. The scatter was not calculated with the bin averaged wind speeds (Figure 3.13a). In contrast the scatter was calculated

with the errors with respect to the linear interpolated power curve (Figure 3.13b), as proposed by
Wagenaar and Eecen (2011) to have a more true approximation.

(a) Not applied   (b) Applied
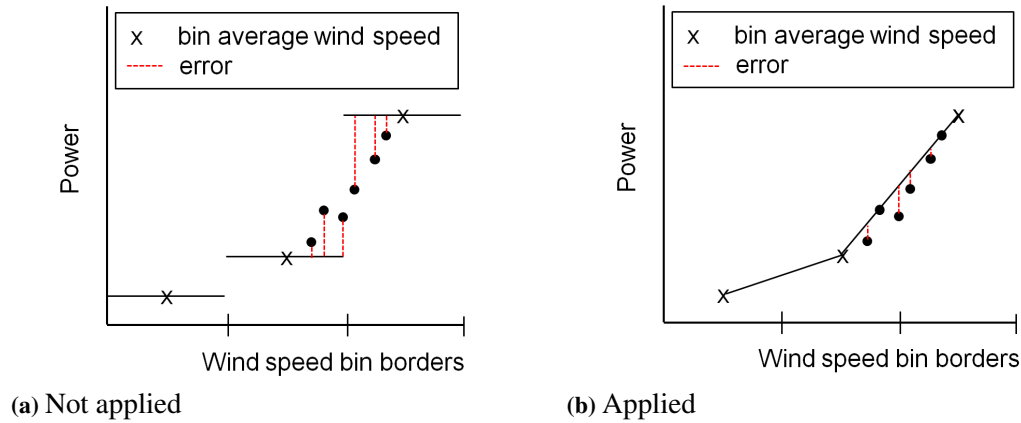
Figure 3.13: Methods for calculating the scatter around a power curve.

3.5.2   Comparing two wind turbines

Having the tool of power performance testing, it was interesting to compare the performance of
the wind turbines where the measurement equipment was installed next to. Fir each wind turbine
its specific undisturbed measurement sectors were used.

3.5.3   Rotor equivalent wind speed

Additional methods could be applied to include the wind speed at multiple heights. Being the
shear correction, which can be supplemented with correction for wind direction.

The wind speed through the whole rotor plane could be taken into account in the Edition 2 stan-
dard, instead of only using the wind speed at hub height. Shear correction was applied using the
rotor equivalent wind speed approach. The rotor equivalent wind speed is the wind speed that
corresponds to the energy flux through the swept rotor area, accounted for the vertical wind shear.
At least 3 heights have to be measured (IEC, 2015). The rotor swept area is divided into multiple
segments as shown in Figure 3.14. The rotor equivalent wind speed can be calculated using:

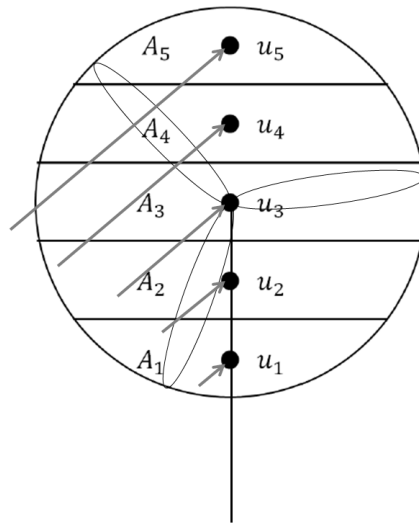$$u_{eq} = \left(\sum_{i=1}^{n_h} u_{10min,i}^3 \frac{A_i}{A} \right)^{1/3} \tag{3.14}$$

Where

n_h is the number of available measurement heights;

$u_{10min,i}$ is the 10 min average wind speed measured at height i;

A is the complete area swept by the rotor;

A_i is the area of the i th segment, i.e. the segment the wind speed u_i is representative for.

Figure 3.14: Rotor swept area divided into segments for rotor equivalent wind speed calcualtion. Figure inpired by Wagner et al. (2011).

The measurement heights for the lidar to calculate the rotor equivalent wind speed were chosen using IEC 61400-12-1 Edition 2. The segments (with areas A_i) are to be chosen such that the horizontal separation line between two segments lies exactly in the middle of two measurement points. The standard illustrates the ideal heights with an example. The example turbine has an hub height of 80 m and a rotor diameter of 100 m, so the lower tip height is 30 m and the upper tip height is 130 m. When choosing 5 measurement heights, they should be evenly distributed at 40, 60, 80, 100 and 120 meter. For the wind turbine under study here, the calculations were similarly performed. We set up the Lidar measurement for 5 heights for the REWS calculation for which the calculations and obtained heights are summarized in Table 3.8 following the method provided by IEC (2015). The segment height was found dividing the diameter by the number of segments, $104m/5 = 20.8m$. The number of segments was chosen to be 5 because a minimum of 3 was requested and 20.8 meter was assumed to be fine enough. The heights then are found by taking the middle of each segment. Table 3.8 shows the measurement heights and the percentage of area covered by each segment.

Table 3.8: Segment weighting A/A_i based on measurement height h_i and lower and heigher limit of the sector (z_i and z_{i+1}).

Segment	h_i (m.a.g.l.)	z_i (m)	z_{i+1} (m)	A_i/A (%)
1	56.4	46	66.5	13.9
2	77.2	66.5	87.5	23.3
3	98	87.5	108.5	25.5
4	118.8	108.5	129.5	23.3
5	139.6	129.5	150	13.9

3.5.4   Veer correction

Correction for changing wind direction with height is proposed in IEC 61400-12-1 Edition 2 by correcting the wind speed in the REWS method with the wind direction. It is assumed that the wind direction at hub height is perpendicular to the rotor plane. The angle between the wind direction at hub height and wind direction at the other heights then is then defined ϕ. The veer correction can be applied using:

$$u_i = u_i * \cos(\phi_i) \tag{3.15}$$

Where
u_i is the wind speed at the segment i, with the segments as in Section 3.5.3; ϕ_i is wind direction at segment i minus the wind direction at hub height.

3.5.5   Inner- versus outer-envelope conditions

For the power performance test of the inner-envelope conditions, turbulence intensity and wind direction measurements are needed to be accurate. For these conditions, the power performance test was analyzed.

3.6   Lidar outages and errors

Unavailability of the Lidar to deliver IEC compliant data can cause longer and more expensive measurement campaigns and could also cause a bias when certain meteorological conditions are always excluded from the measurements. Therefor the duration of unavailability and its causes are explored.

Outages were found by counting the amount of 10-minute entries in the Zephir data-file. When there was an outage there were simply no rows in the CSV file. With 144 10-minute intervals in a day, the ratio of outages was calculated as $(144 - entries)/144$. Equally, the errors per category were counted.
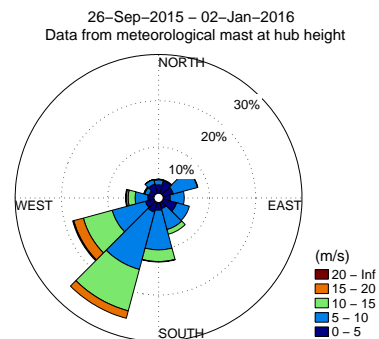
Chapter 4

Meteorological conditions at the site

The wind conditions at the site are shown in Figure 4.1. The Weibull fit closely approximates a Rayleigh distribution function and the prevailing wind direction is from South-West. The mean wind speed is higher than the average wind speed when all data since the measurements of the meteorological mast started on February 3, 2015. The prevailing wind direction is similar. Figures including historical data starting before this measurement campaign are shown in Figure B.1.

More detailed information on the wind profile can be found in Section E.
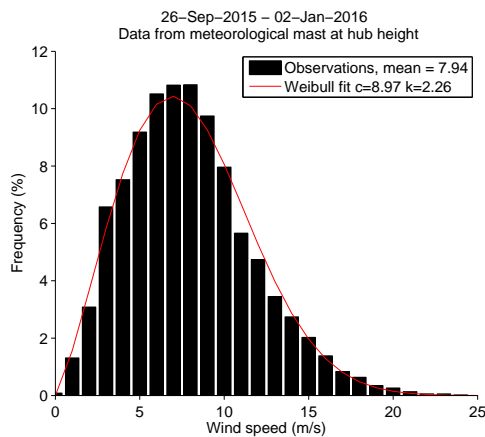
(a) Wind speed distribution   (b) Wind rose

Figure 4.1: Wind conditions at the site.

Chapter 5

Lidar measurement validation

In this chapter the Lidar measurements are validated against the IEC compliant meteorological mast. These measurements needed for power performance testing are the wind speed, turbulence intensity (for guaranteed power curves condition selection) wind direction, air pressure, temperature and relative humidity. Note that the wind speed and direction are measured on a larger volume by the Lidar than for the meteorological mast which measures more or less a point volume. Furthermore the Lidar measures the air pressure, temperature and relative humidity at 1 meter above ground level which had to be corrected to hub height.
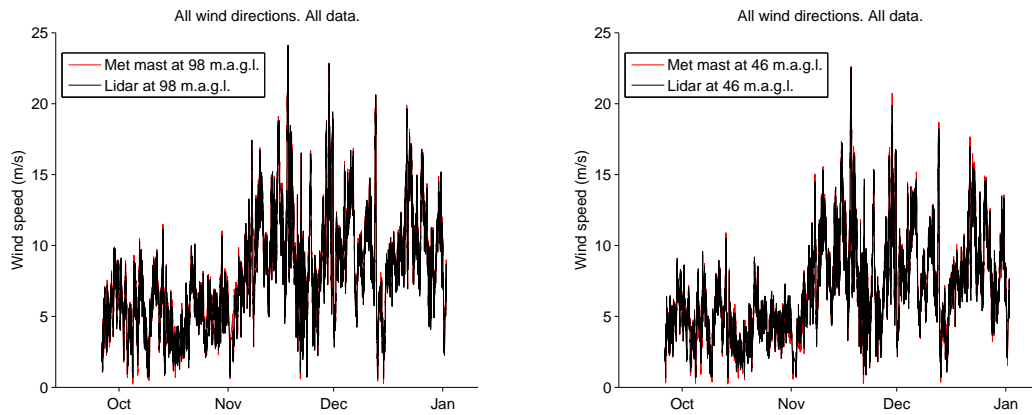
5.1   Wind speed

Figure 5.1 shows an first impression on the wind speed measurements of the Lidar. The wind speed measurements at different heights show that the Lidar measures mostly higher wind speeds at higher heights, as could be expected.
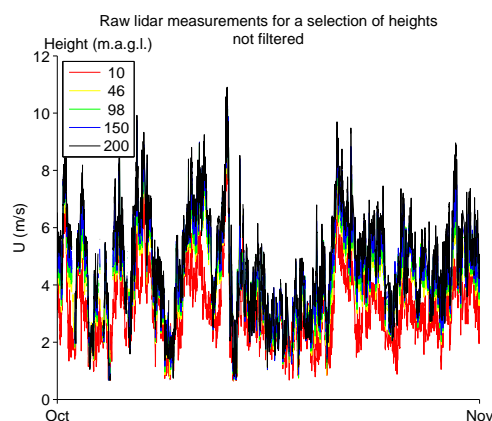
**Figure 5.1:** Lidar wind speed measurements at some heights.

The comparison with the meteorological mast is shown in Figure 5.2. On first sight it becomes

apparent that the measurements of the Lidar coincides well with those of the meteorological for both heights.
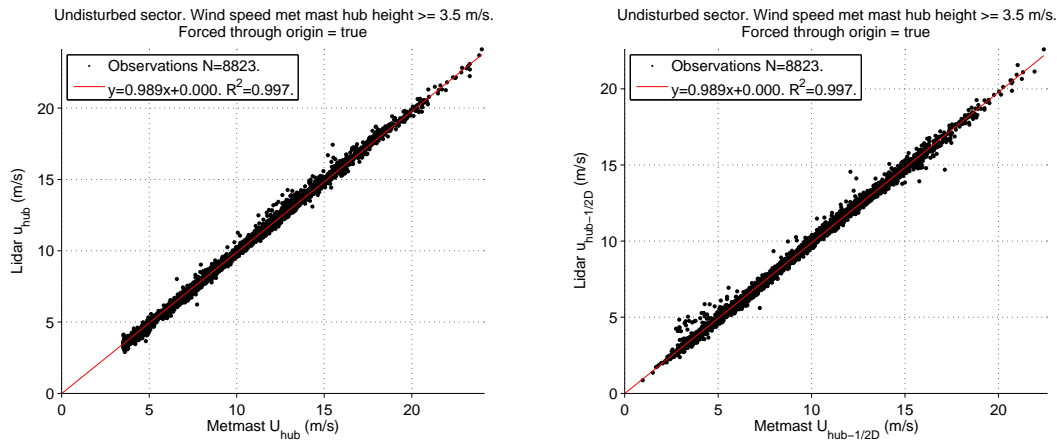

Figure 5.2: Wind speed.

The linear regression for the wind speeds is shown in Figure 5.3. For the power performance measurements, we zoom in to wind speeds above cut-in wind speed at hub height of the meteorological mast. Some data points below cut-in wind speed are apparent for the 46 meter above ground level plot, because the data was filtered using the hub height wind speed. The wind speed at 98 meter, shows good comparison. At 46 meter, there is a larger difference in wind speeds. This could be due to the fact that there is only one anemometer at that height on the meteorological mast, which can suffer from flow distortion of the meteorological mast as explained in Section 3.2.1.
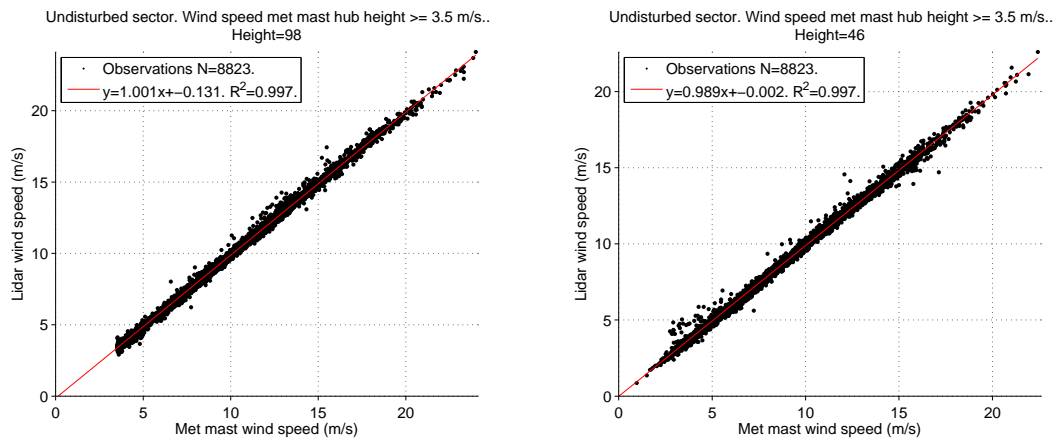
Figure 5.3: Wind speed linear regression (not forced through the origin).

Figure 5.4: Wind speed linear regression forced through origin, as done for the Norsewind criteria.

In order to understand whether the wind speeds are measured as correctly according to a broad range of stakeholders in the wind industry, the Norsewind criteria are tested in Table 5.1 (as explained in Section 3.4.1). All criteria were met. The regression is forced through the origin as shown in Figure 5.4. The slope < 1 depicts that the average wind speed measurement by the Lidar is lower than that of the anemometers at the meteorological mast, for all wind speed categories. The regression R^2 shows that there is a high fit.

Table 5.1: Norsewind criteria for undisturbed wind sector. Forced through origin and starting from windspeed of 3 m/s. Category wind speeds (m/s) are measured in as measured from the meteorological mast; at 98 meter by the anemometer not disturbed by the meteorological mast, at 46 by the single anemometer at that height.

| Criteria	Category	Threshold	98m	Pass 98m	46m	Pass 46m
Valid data points (#)	3.5<=u<8	>=500	3071	True	4318	True
	8<=u<12	>=500	3813	True	2962	True
	all u>=3.5	>=500	8823	True	8463	True
Ratio abs(err) $\geq$ 0.5 m/s	all u>=3.5	<0.10	0.008	True	0.005	True
a	3.5<=u<8	0.98<= a <1.02	0.980	True	0.986	True
	8<=u<12	0.98<= a <1.02	0.987	True	0.992	True
	all u>=3.5	0.98<= a <1.02	0.989	True	0.989	True
b	3.5<=u<8	Not defined	0.000		0.000	
	8<=u<12	Not defined	0.000		0.000	
	all u>=3.5	Not defined	0.000		0.000	
$a_{8-12m/s} - a_{3-8m/s}$		<0.015	0.007	True	0.006	True
Linear regression R^2	3.5<=u<8	>0.98	0.985	True	0.984	True
	8<=u<12	>0.98	0.981	True	0.981	True
	all u>=3.5	>0.98	0.997	True	0.997	True

5.2 Air density

The air density as measured using the meteorological mast and meteorological station at the Lidar are shown in Figure 5.5. The correlation for air density is much worse than for wind speed but it should be kept in mind that air density is far less of influence for the power in the wind than the wind speed (Equation 2.5).

The height correction is clearly of large importance. However, especially the more extreme values of the the air density seem not to be found correctly by the Lidar its meteorological station. The underlying parameters, air temperature, air pressure and relative humidity are shown in Section C, which shows that the pressure is measured very well, but the air temperature is mainly causing the differences. A possible explanation could that the temperature at 1 meter above ground level is influenced by the ground, which has embodied energy and could emit heat while the air is colder. Then at 1 meter above ground level, the temperature could be higher than that at 98 meter, while the correction would give a lower temperature at 98 meter (with the negative temperature gradient in Equation 3.5).

Figure 5.6 shows that the (height corrected) air density has a large scatter, and scatter is much larger than the scatter in wind speed measurements (e.g. R^2 is smaller than in Figure 5.2).

(a) Not corrected to height

(b) Corrected to height
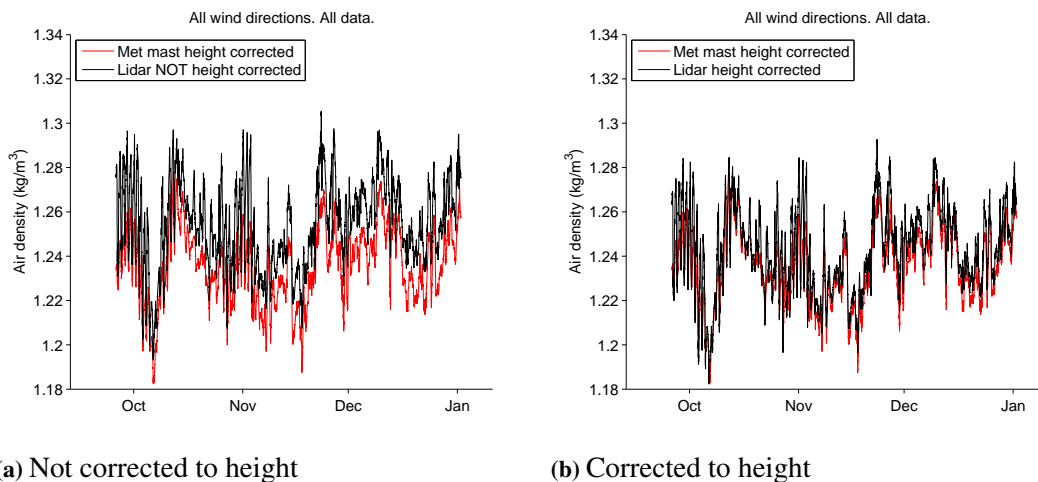
Figure 5.5: Air density.
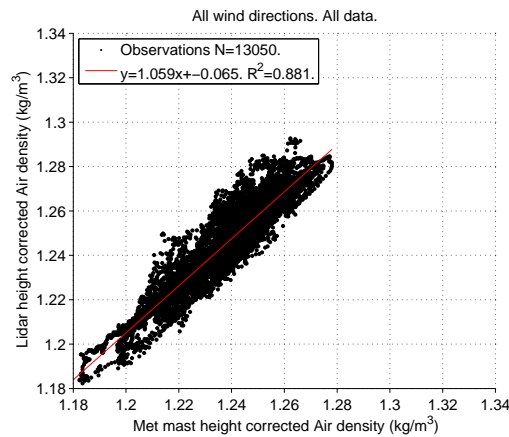
Figure 5.6: Air density linear regression.

5.3 Wind direction
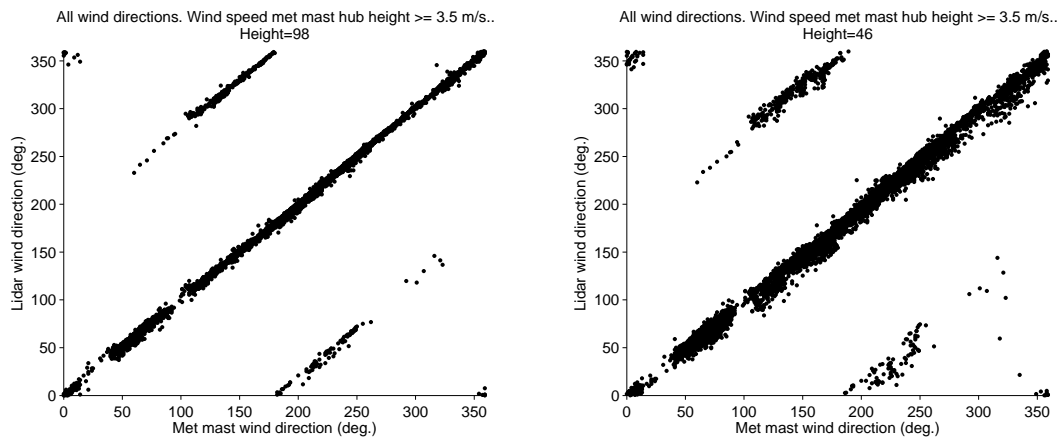
5.3.1 Measured wind direction

The first insight in the wind speed comparison is shown in Figure 5.7. The wind direction measurements at both heights seem to coincide pretty well on this scale for the largest share of the time. However mainly in end September and October there are some clear differences.
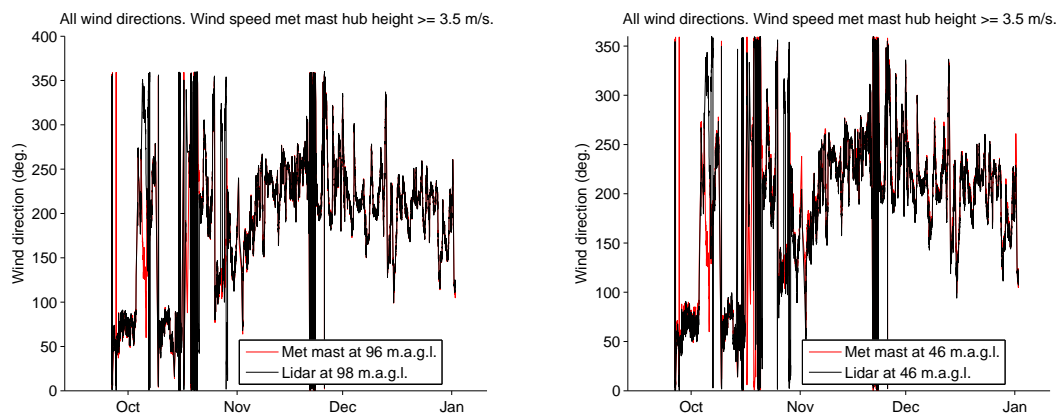

Figure 5.7: Wind direction time series.

When the Lidar wind direction measurements are off by more than a few degrees, the difference in measurement is often approximately 180 degrees (Figure 5.8).

Figure 5.8: Wind direction scatter. Data is included for wind speeds relevant for power performance measurements.

The Lidar wind direction measurement ambiguity of 180 degrees is resolved by using the meteorological station at the Lidar (as discussed in Section 2.1.2). The meteorological station does not give accurate measurements, because there is flow distortion by the fence around the Lidar and also by the generator that is positioned at a few meters distance (Figure 5.9). However, when the Lidar would use the wind direction correction directly it would be expected that the wind direction of the Lidar would be corrected always when the difference between the Lidar measurement and meteorological station at the Lidar is more than 90 degrees. However this hypothesis is not confirmed as depicted in Figure 5.10. After a phone call with the manufacturer (Lewis, 2016) it became clear that the wind direction measurement indeed is dependent on the meteorological station, however that the direction is not obtained directly. A time delay function is build in for the wind direction calculation. Both the previous wind direction measurements and current wind direction measurements are used as input to determine the current wind direction. Only after a while the meteorological station data is able to convince that the wind direction at the moment is 180 degree different than the current output. A reason for this is to prevent flow distortion for the flow on the meteorological station of the Lidar have too large influences.
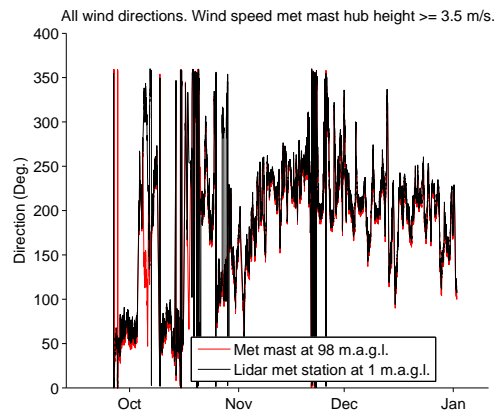
**Figure 5.9:** Wind direction measured by meteorlogical station at the Lidar.
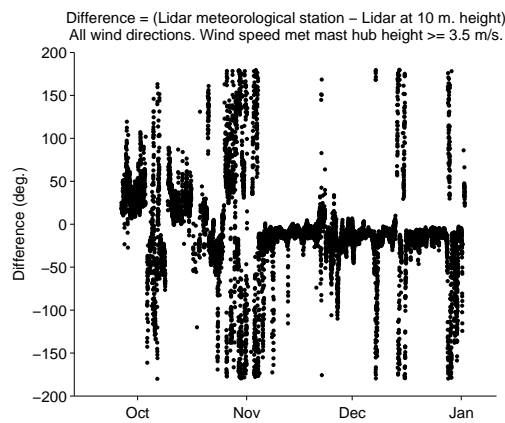
Figure 5.10: Wind direction difference between meteorological station at the Lidar and wind direction of the Lidar at its lowest measured height.

5.3.2 Adjusted wind direction

It is checked whether the wind direction measurement errors could be corrected for, because the Lidar measuring the wind direction sometimes approximately 180 degrees off. Namely, for the power performance tests, this would be needed to exclude the data where the flow is coming from directions with a disturbed wind flow (IEC, 2005).

The wind direction is accurately measured with the wind turbine when a filter is applied. Firstly excluding the times where the wind turbine gives an error (as would be done too when a power performance measurement is done). Secondly excluding all times where the wind direction as measured by the wind turbine is 0 degrees, thus precisely North. These measurements were excluded because most of them were obvious erroneous measurements by the wind vane at the wind turbine. The correlation is shown in Figure 5.11a. The wind direction was adjusted by adding 180 degrees to the Lidar measurements when the absolute difference between the Lidar and the wind

turbine was more than 90 degrees (5.11b). The corrected wind direction has a good fit. The advantage of Lidar measurements, compared to only the wind turbine wind direction measurements is that a wind shear correction could be applied (Section 3.5.4).

(a) Wind turbine measurements   (b) Lidar corrected using wind turbine
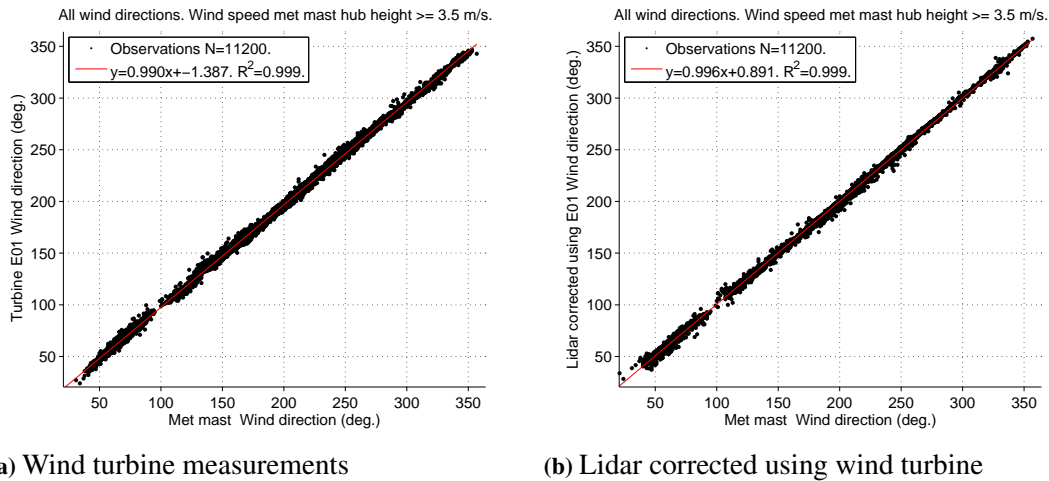
Figure 5.11: Lidar wind direction measurements corrected using wind turbine E01.

5.4   Turbulence intensity

Turbulence intensity for wind speeds ≥ 3.5 m/s are plotted as time-series in Figure 5.12. With the large fluctuations it is difficult to see how well the Lidar measures the turbulence intensity. Using a linear regression analysis in Figure 5.13, it can be observed that there is a large scatter. The Lidar measures turbulence differently than the meteorological mast. For the Lidar a height is scanned and then the next height is scanned and also turbulence could be estimated using the fit of the wind speed its R^2. Also there are discussions on how well a cup anemometer can measure turbulence.
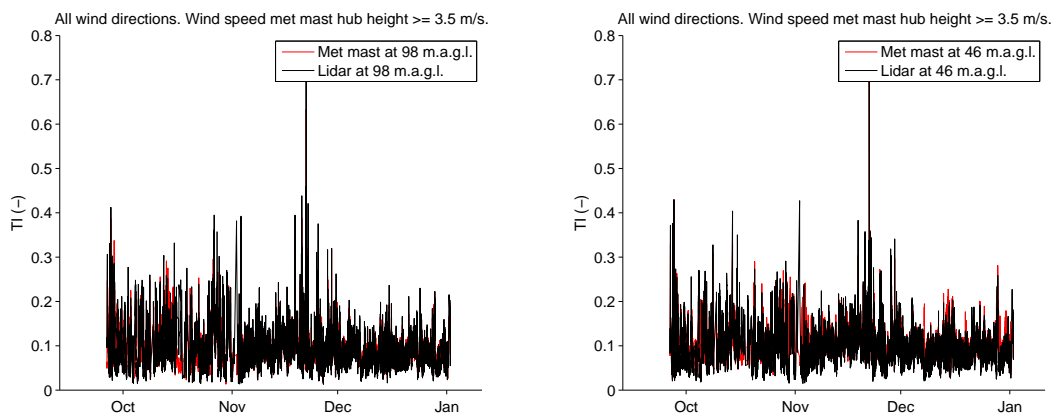
Figure 5.12: Turbulence intensity.
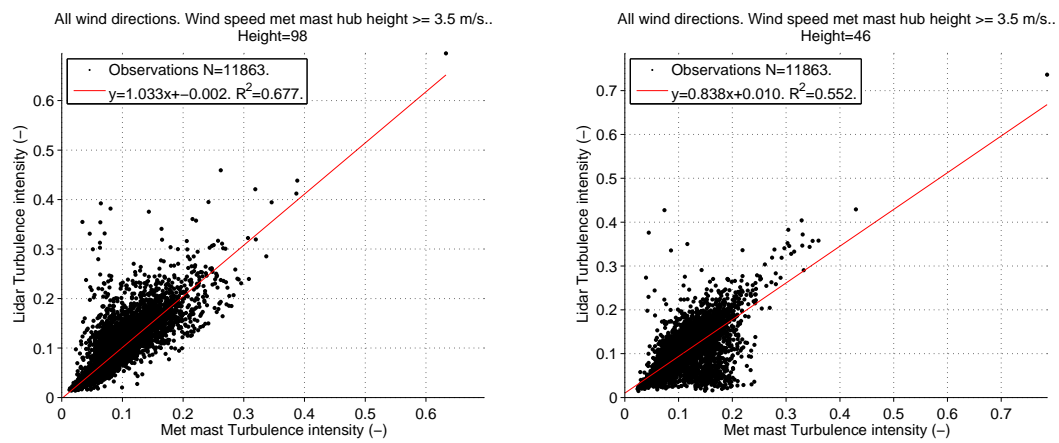
**Figure 5.13:** Turbulence intensity linear regression.

Chapter 6

Power performance tests

Multiple power performance tests are performed. At first, hub height measurements of the Lidar and meteorological mast are compared, then the power performance of two wind turbines is compared. Thereafter, the rotor equivalent wind speed and veer methodologies are implemented. Lastly the wind turbine performance for inner- and outer envelope conditions are compared.
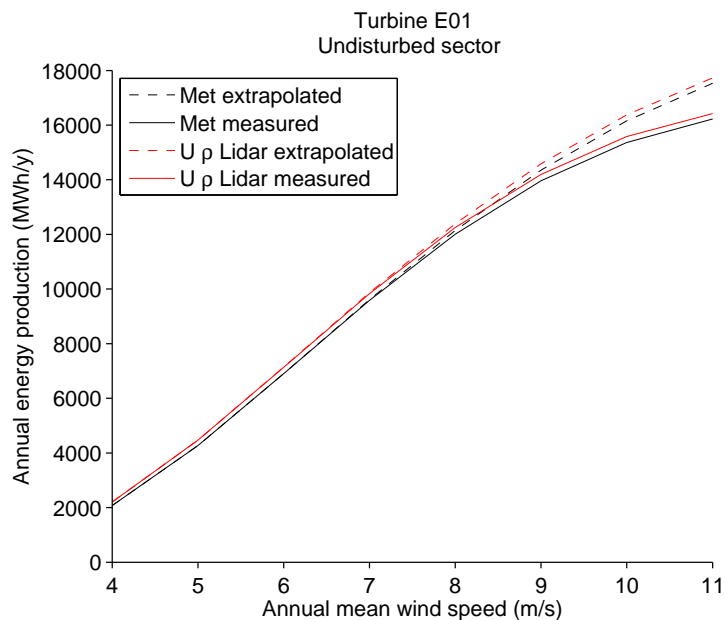
6.1 Meteorlogical mast and Lidar at hub height

The power performance of measurements using the meteorological mast or using the Lidar are compared in Figure 6.1. The wind speed measurement has a larger impact than the air density measurement on the difference in power performance (Equation 2.5). Measuring a lower wind speed with the Lidar makes that the power curve looks 'better' because the same amount of energy is generated but for a lower wind speed. When adding the wind speed distribution over the year and calculating the AEP, the difference is large, more than two percent for an annual mean wind speed of 7 m/s (Figure 6.2 and Figure 6.3).
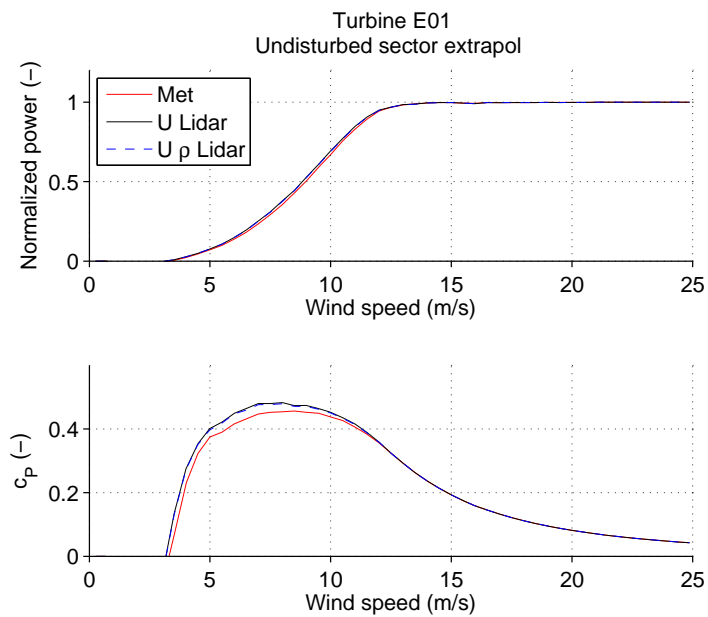
Figure 6.1: Meteorological mast versus Lidar power curve and power coefficient. For the Lidar using only Lidar wind speed or Lidar wind speed and air density calculated from its meteorological station corrected to height.

The difference in AEP is shown in Figure 6.2 and the difference in AEP is shown in Figure 6.3. The difference in AEP seems to be more or less continuous over all annual mean wind speeds.


Figure 6.2: AEP with hub height measurements of Lidar and meteorological mast.
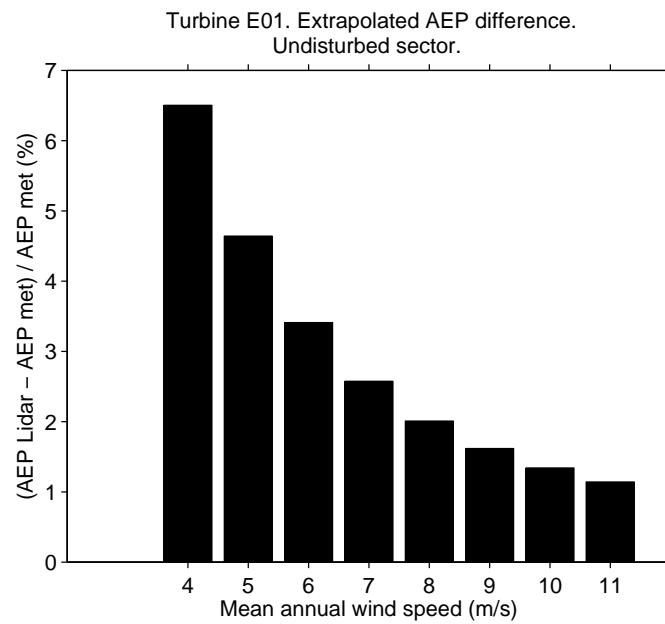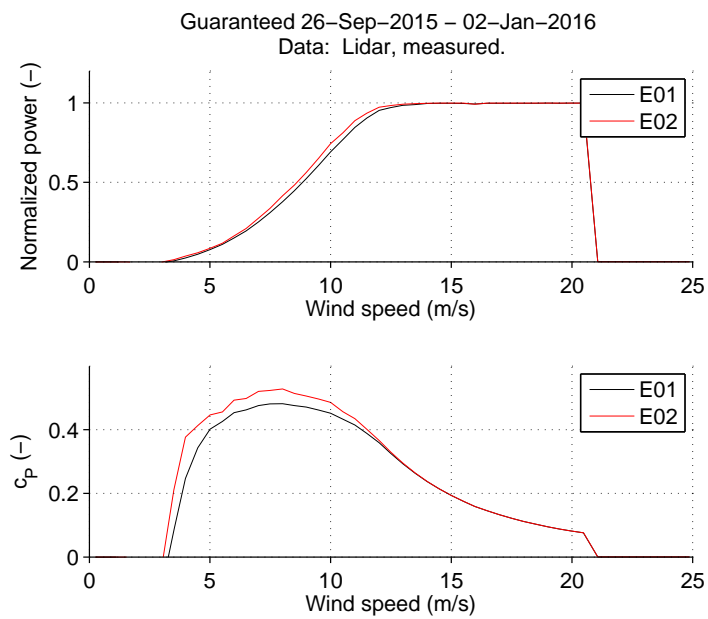
Figure 6.3: AEP difference.

6.2   Comparing two wind turbines

Turbine E01 and E02 could be compared for power performance using the meteorological mast and the Lidar. Turbine E01 clearly performs less good than Turbine E02. This effect can clearly be seen using the meteorological mast (Figure 6.4) or using the Lidar (Figure 6.5). The AEP comparison in with the Meteorological mast (Figure 6.6 and Figure 6.8) are comparable with those using the Lidar (Figure 6.7 and Figure 6.9). This result was expected because the Lidar and meteorological mast measurements showed a low scatter compared with respect to each other.
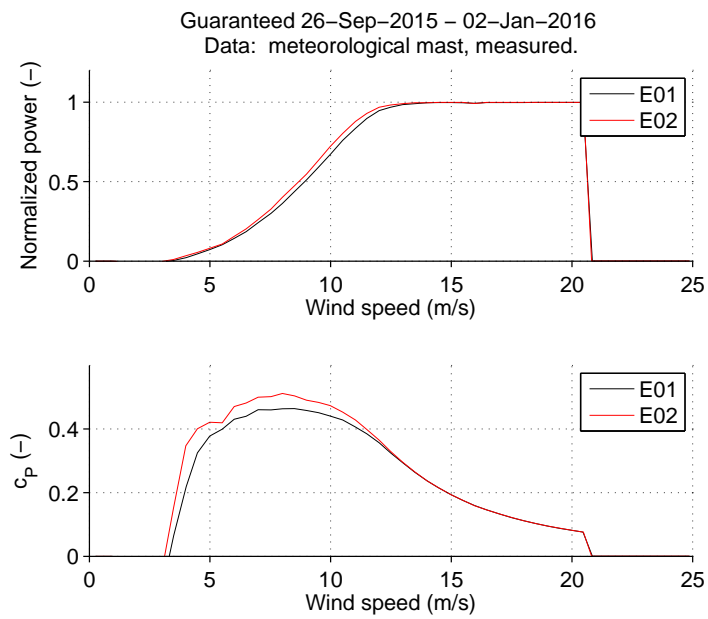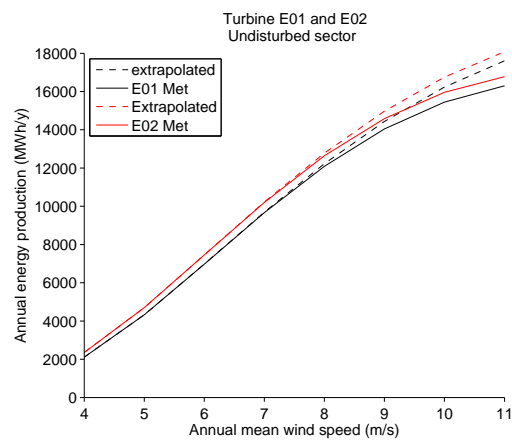
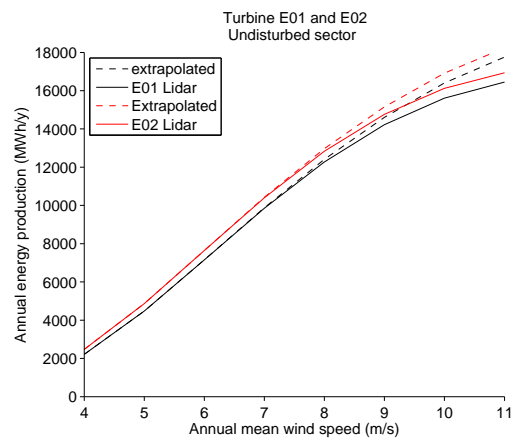**Figure 6.4:** Wind turbine E01 and E02 comparisson using meteorological mast.

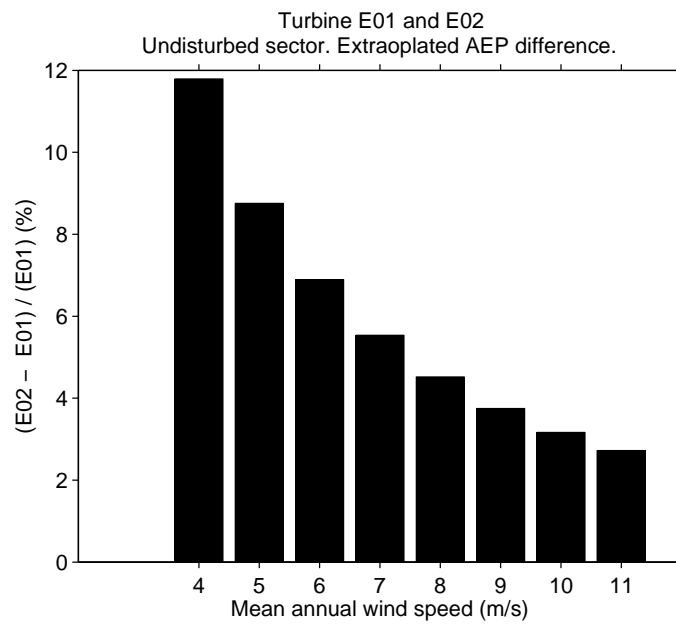**Figure 6.5:** Wind turbine E01 and E02 comparisson using Lidar.

Figure 6.6: AEP calculation using meteorological mast.

Figure 6.7: AEP calculation using Lidar.

Figure 6.8: AEP difference using meteorological mast.
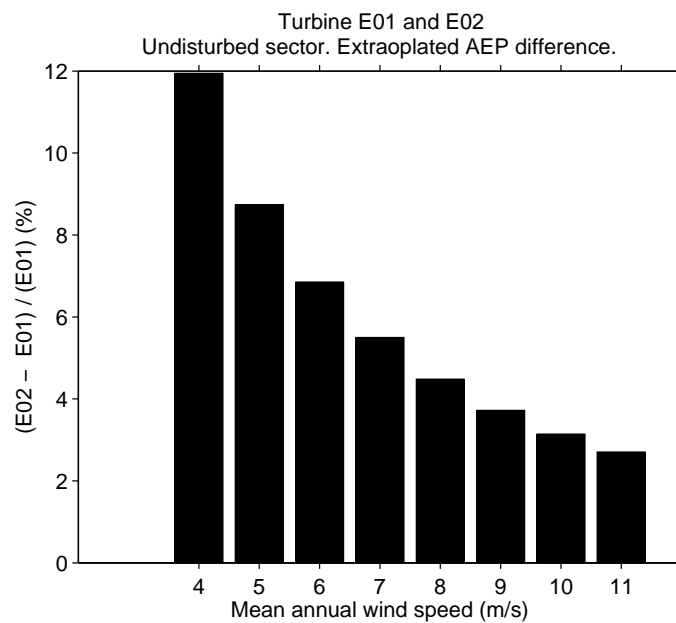
Figure 6.9: AEP difference using Lida.r

6.3   Rotor equivalent wind speed

The linear regression of the wind speed at hub height and rotor equivalent wind speed, shows that there is a difference for this measurement campaign (Figure 6.10).

The power curves are compared in Figure 6.11 and AEP is compared in Figure 6.13 and more

clearly seen in Figure 6.14. The comparison is made to show the impact of the calculations. However, a comparison for power performance testing between a REWS and hub height method would never be drawn in one graph, because the underlying wind speed is different (the yearly mean rotor equivalent wind differs form the yearly mean wind speed at hub height). The AEP difference is approximately 0.5 % during this measurement campaign. The change in scatter around the power curve was checked for in Figure 6.12. The scatter reduces slightly compared to hub height measurements using the Lidar, but the scatter using the meteorological mast is lower.
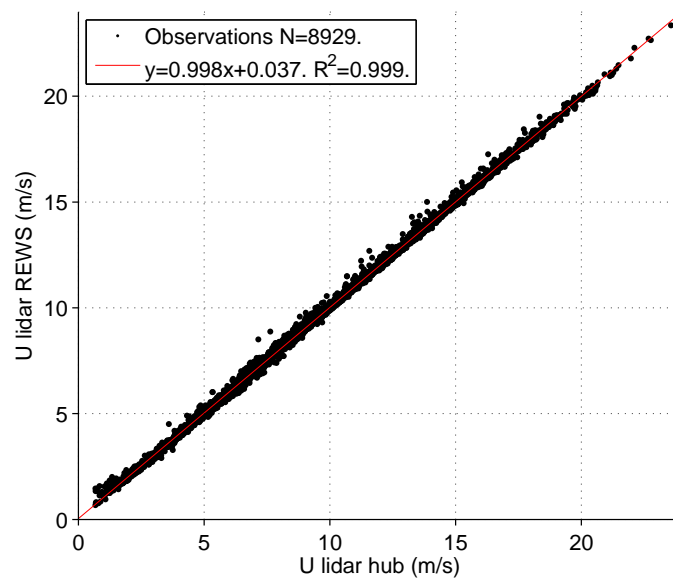
Figure 6.10: Linear regression for REWS versus hub height wind speed measured by the Lidar.
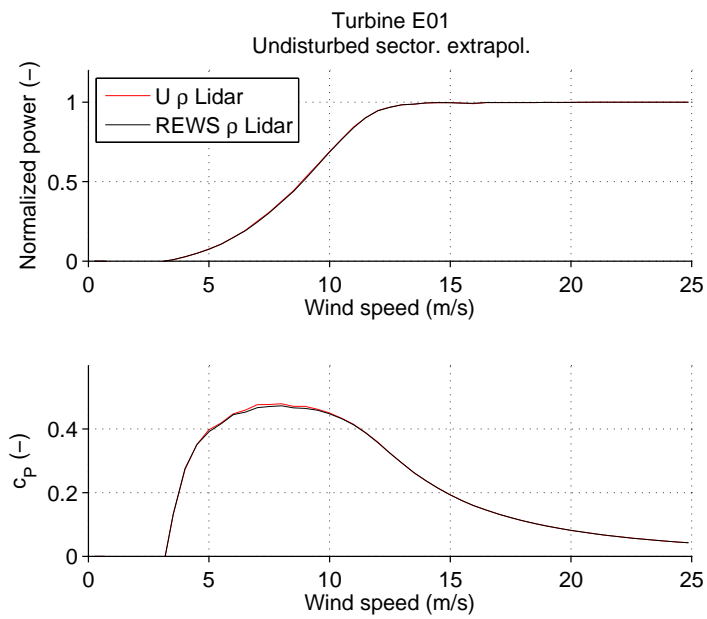
Figure 6.11: Rotor equivalent wind speed power curve compared to hub height wind speed power curve.
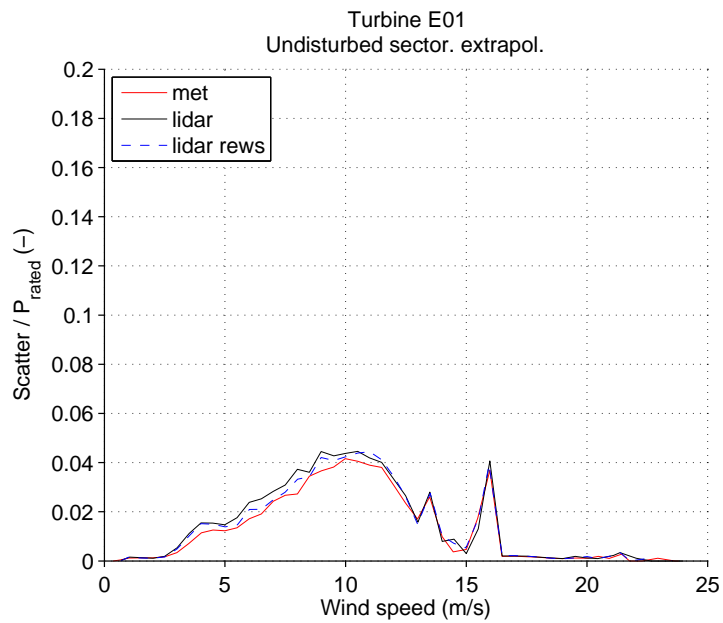
Figure 6.12: Scatter around the mean power curve for different wind speed measurement methods.
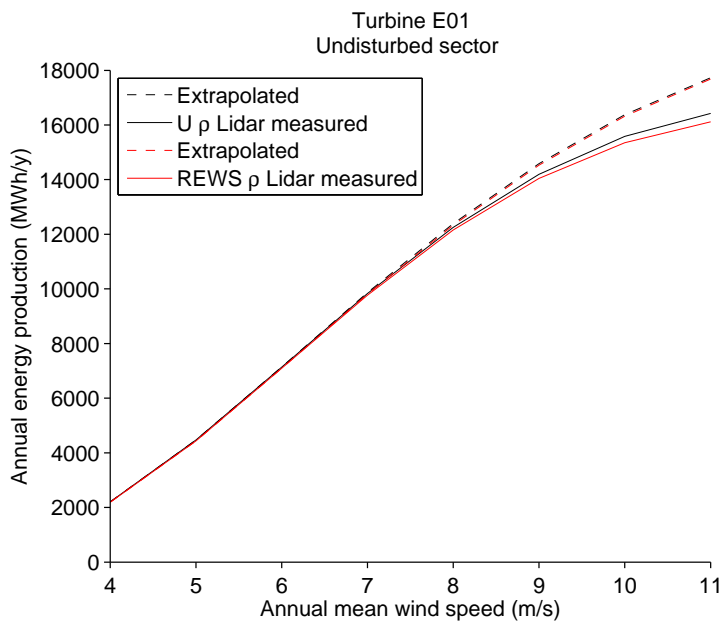
Figure 6.13: AEP Lidar hub height and Lidar REWS.
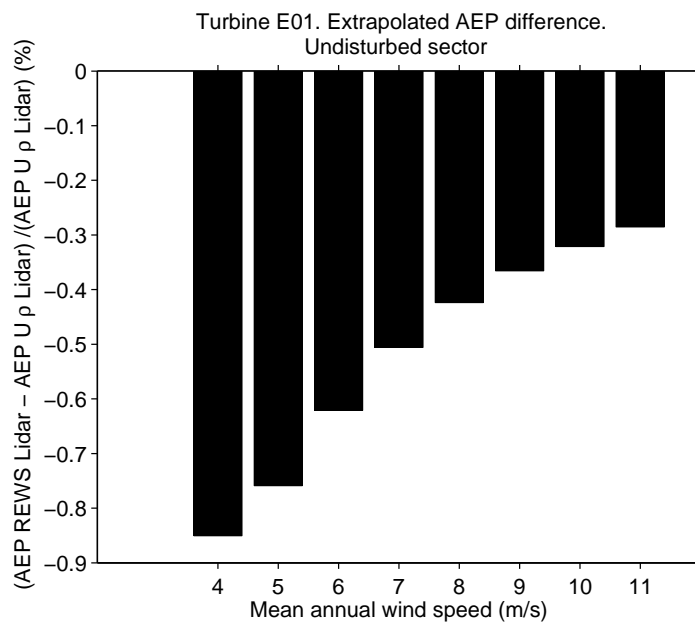
Figure 6.14: Difference in AEP Lidar hub height and Lidar REWS.

6.4 Veer correction

Veer correction is applied (correcting the wind speed for the varying wind direction with height).
This correction is applied on top of the REWS method. The difference in wind direction with
height is small, such that correcting for veer does not show a large difference for this measurement

campaign(Figure 6.15, Figure 6.16 and Figure 6.18).

The difference in scatter is shown in Figure 6.17. Again it shows hardly any difference with the rotor equivalent wind speed method.
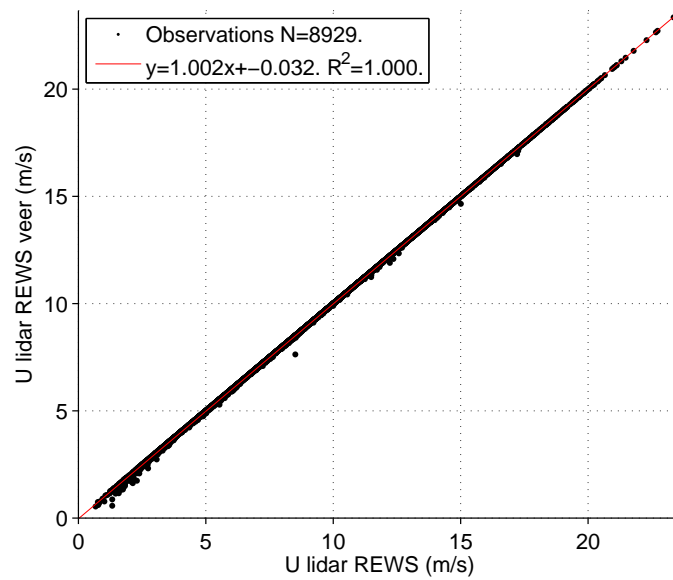
Figure 6.15: Veer corrected wind speed versus REWS wind speed
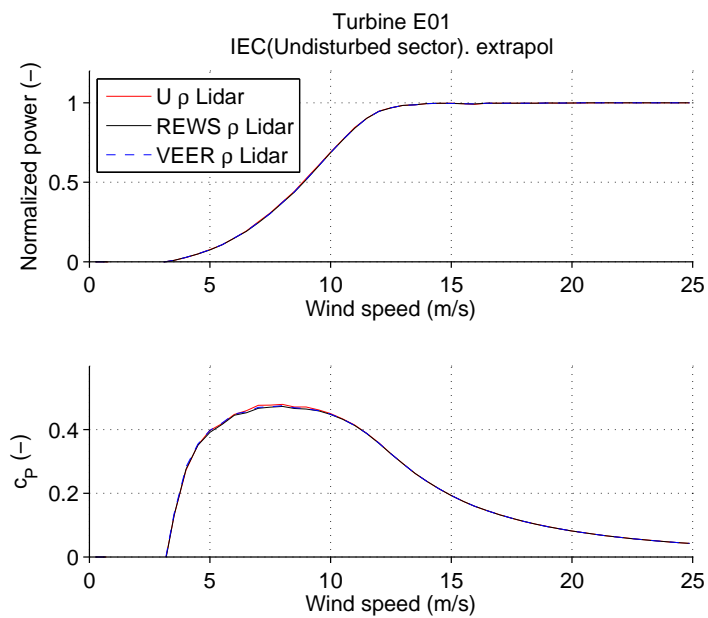
Figure 6.16: Veer corrected power curve compared to REWS power curve and hub height wind speed power curve.
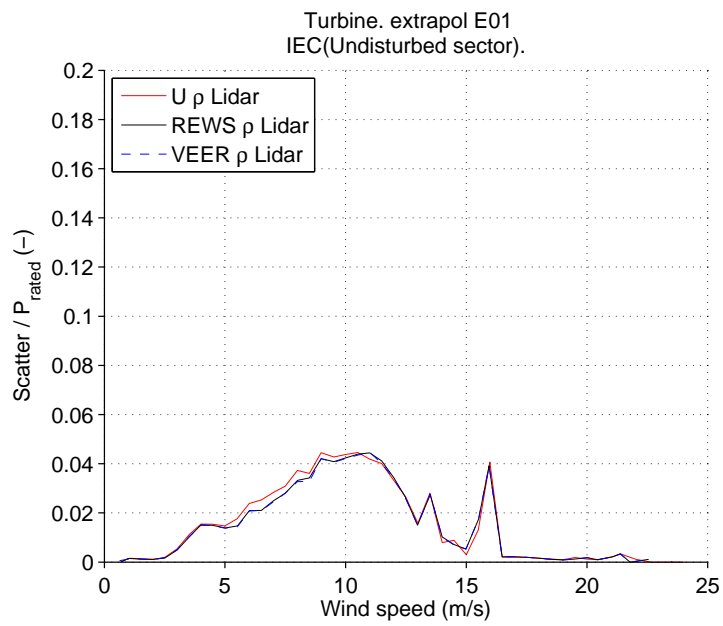
Figure 6.17: Scatter of veer corrected wind speed versus REWS wind speed.

Figure 6.18: Difference in AEP Lidar REWS and Lidar veer.

6.5 Inner- versus outer-envelope conditions

6.5.1 Time

The inner-envelope conditions for the guaranteed power curve only occur for a small part of the time as shown in Figure 6.19. It should be noted that in this figure the order of applying filtering matters. First we exclude the wind speeds that are below cut-in wind speed, as these are not of influence for the power performance calculations. Thereafter the direction, hysteresis, fault and temperature conditions are part of the IEC filter. It can be seen that the direct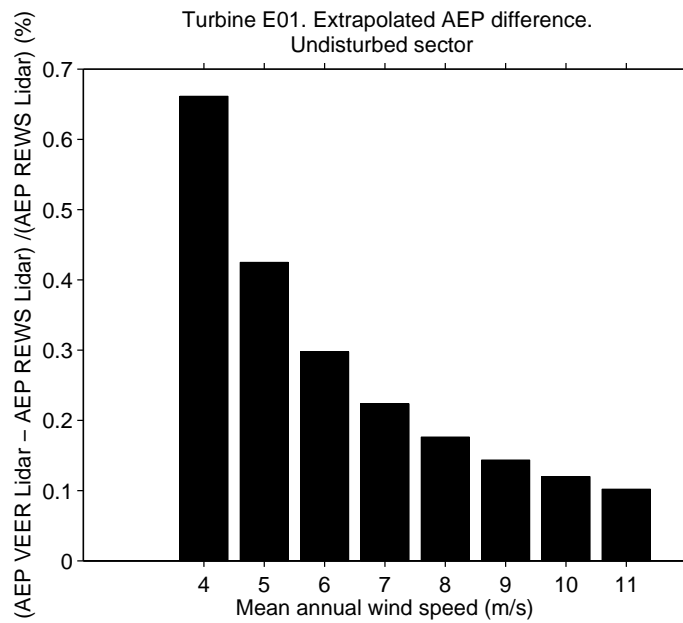ion has the largest filtering where a the data can not be used because the wind flow is distorted by surrounding objects. For going from IEC conditions to inner envelope conditions, the shear, turbulence intensity and air density come into play (as was summarized in Table 3.2). Turbulence intensity and wind shear have the largest impact and air density has no impact.

In Figure 6.19 the order when filtering is applied plays a role. When not using this order, data is less easy to interpret but gives extra insights (Table 6.1). Wind shear and turbulence intensity are often both in outer envelope conditions. This is furthermore shown in Figure 6.20. In this figure inner and outer guaranteed power curve conditions for wind shear and turbulence are shown. The ratio between inner envelope conditions and outer envelope conditions is similar to that found by Wessels (2015) for the Princess Alexia wind farm over the period February 3, 2015 until July 7, 2015.
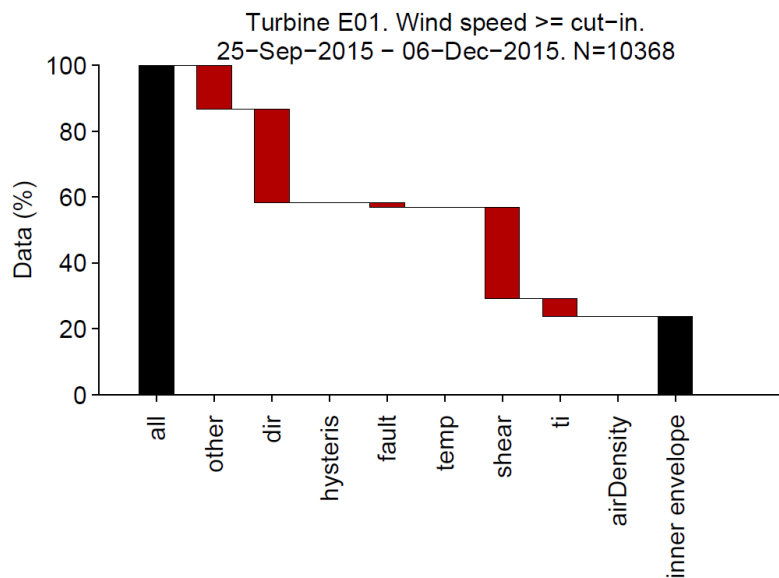
Figure 6.19: Percentage of time that inner and outher envelope conditions occur.'Other' means that only wind speed >= cut-in wind speed (3.5 m/s) is kept.

Table 6.1: Percentage of data that is kept included per filter variable. 'Other' means that only wind speed >= cut-in wind speed (3.5 m/s) is kept.

	IEC / total (%)	Inner envelope / total (%)
other	86.6	86.6
dir	64.0	64.0
hysteris	100.0	100.0
fault	97.8	97.8
temp	99.5	99.5
shear	100.0	50.2
ti	100.0	62.1
airDensity	100.0	100.0
total	56.7	23.6
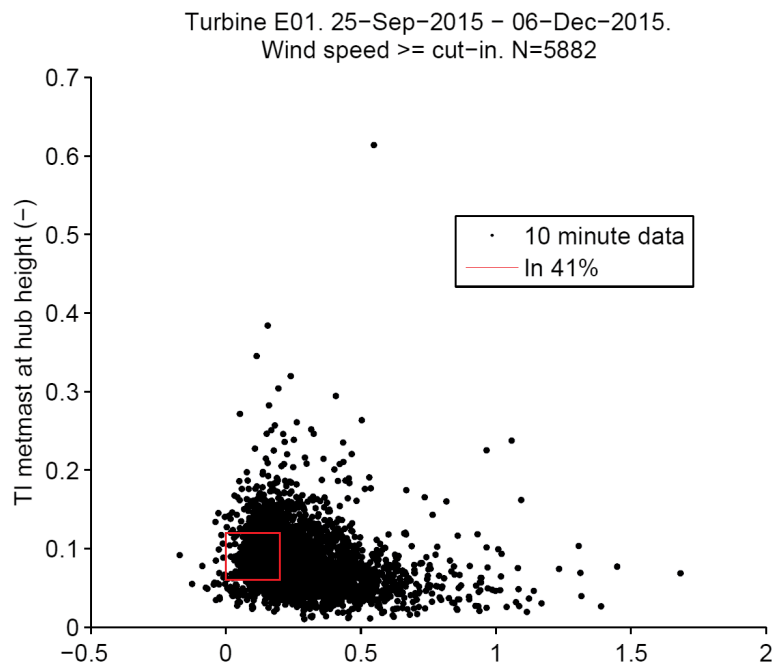
Figure 6.20: Inner- versus outer envelope guaranteed power performance conditions. The value of inner versus outer power curve conditions is found by dividing the ratio of guaranteed/total by IEC/total. Visualization based on Wessels (2015).

6.5.2 Power curve and AEP

The data for the guaranteed power curve is shown in Figure 6.21. It already can be seen that the guaranteed power curve shows less scatter. Furthermore, when taking the average power per bin, the power curve shows comparable characteristics in Figure 6.22. The extrapolated power curve is shown, so that the influence of less than 3 data points is not distracting too much for wind speeds higher than rated wind speed.

(a) Inner+outer envelope
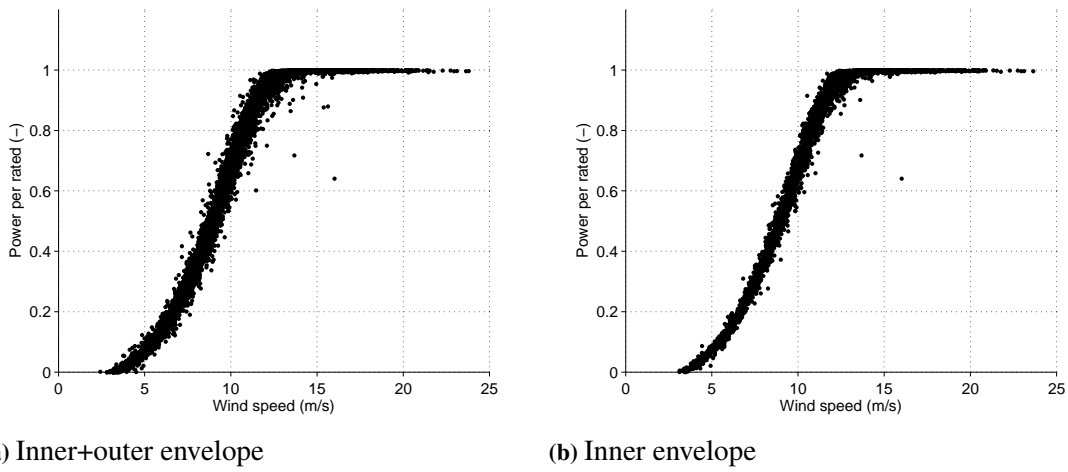
(b) Inner envelope

Figure 6.21: Comparisson of inner and outer envelope power curve data.

(a) Power curve

(b) Scatter
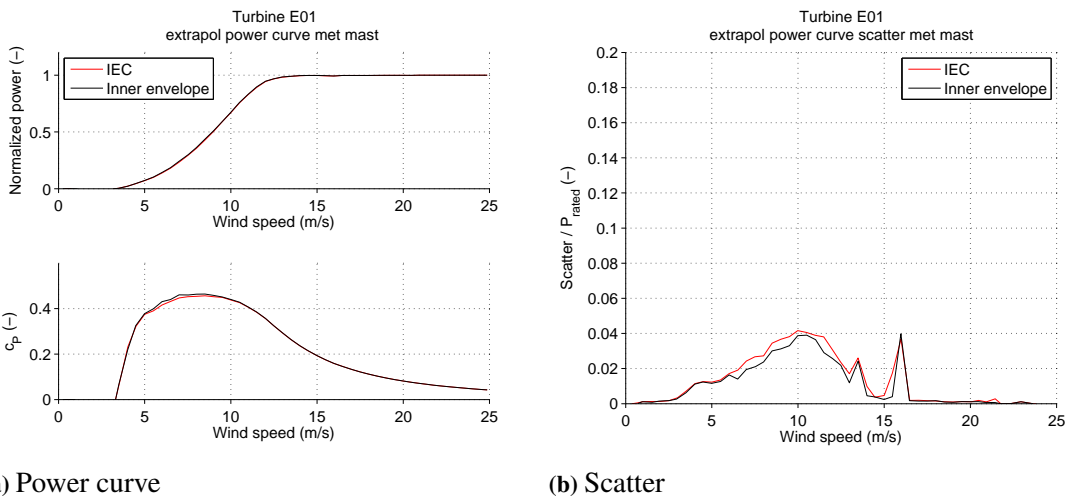
Figure 6.22: Inner and IEC envelope comparisson. For extrapolated power curve.

The in inner- and outer AEP conditions are compared in Figure 6.23 and its difference is more clearly seen in Figure 6.24. The difference in inner and outer AEP conditions is shown in Figure 6.24.
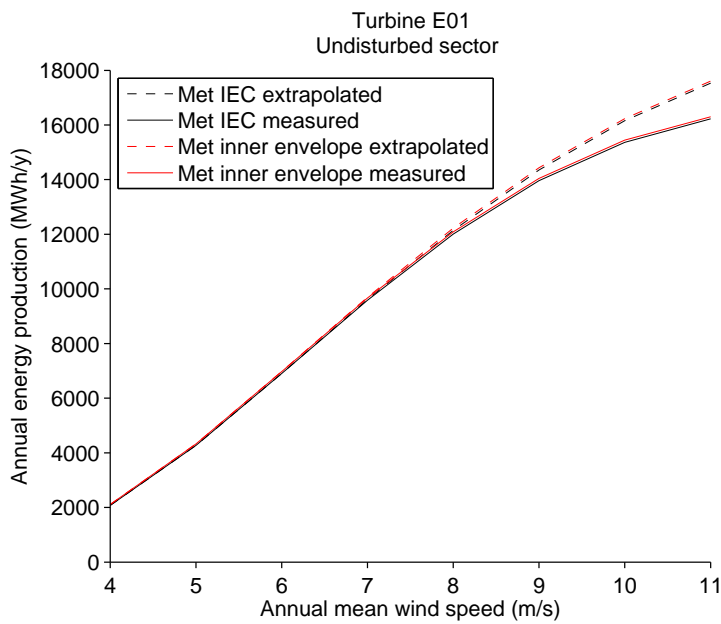
Figure 6.23: AEP for inner- and outer envelope conditions.
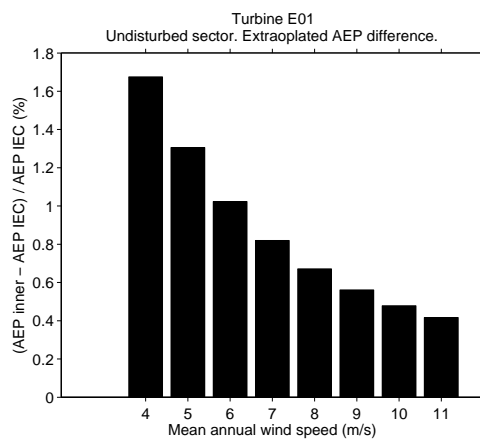
Figure 6.24: Difference in AEP for inner and inner+outer envelope conditions.

It is tested whether the measured power curve is valid for estimating the AEP with a mean annual wind speed of 7 m/s for the Rayleigh probability distribution function of the wind speed versus time. Since the difference is less than 95% as shown in Table 6.2, the AEP estimation is valid (IEC, 2005).
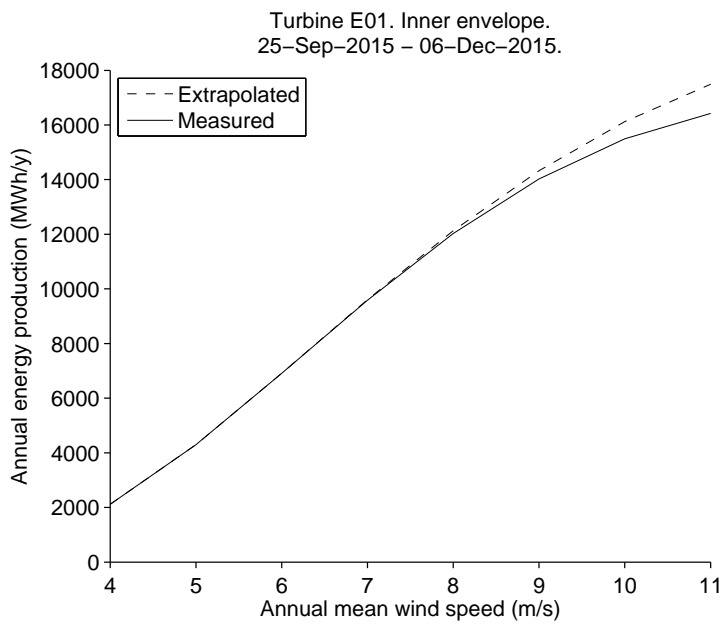
Figure 6.25: AEP measured versus AEP extrapolated for inner envelop conditions.

Table 6.2: AEP measured versus AEP extrapolated and validity check of AEP calculation for different mean yearly wind speeds.

U (m/s)	Measured (MWh/y)	Extrapolated (MWh/y)	Ratio (%)	Complete
4	2120	2120	100	1
5	4296	4296	100	1
6	6910	6911	100	1
7	9587	9607	100	1
8	12025	12127	99	1
9	14024	14326	98	1
10	15491	16124	96	1
11	16426	17490	94	0

Chapter 7

Lidar outages and errors

An error analysis is performed with the goal to understand if these cause increased measurement periods for a power performance verification. For a power performance test, it is needed to have data for each requested wind speed bin as explained in Section 3.5.1.

Lidar unavailability can be categorized as outages or as errors outputted by the lidar software. Errors as outputted by the lidar software are due to the quality control "to meet IEC compliance and provide financial grade data" according to the ZephIR 300 data analysis guide (ZephIR, 2015a). The outages and errors are defined hereunder.

Outages are defined as missing data, for example due to malfunctioning hardware or installation problems.

Error 9998 is defined in the ZephIR 300 data analysis guide as "[t]he ZephIR automatically detects atmospheric conditions which adversely affect lidar wind-speed measurements. For example, in thick fog the beam from a lidar device may not be able to reach the measurement height. Also in certain cases when affected by significant precipitation, the ZephIR will also reject the vertical component of the wind speed and only vertical wind speeds – horizontal speeds are unaffected by rain" (ZephIR, 2015a).

Error 9999 is defined by the ZephIR as "[h]igh quality wind speed measurement is not possible. This is often caused by very low wind speed, or due to partial obscuration of the ZephIR window, or significant interference with the laser beam at the specified height" (ZephIR, 2015a).

Errors at at least 1 REWS height
All data
26−Sep−2015 − 02−Jan−2016 N=14113
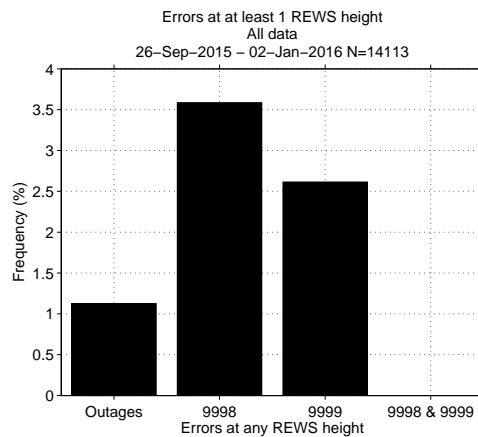
Figure 7.1: Overview of outages and errors.

Figure 7.1 summarizes the outages and errors during the measurement period. Most of the data incompleteness is caused by Error 9998. Errors are counted for the moments that the measurement can not be used for the REWS calculation anymore, thus that any of the measurements at 56, 77, 98, 118 or 139 meter above ground level has an error.
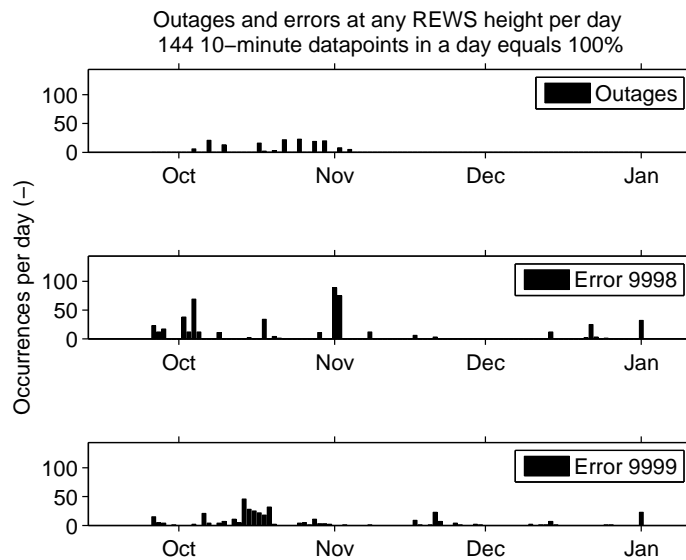
Figure 7.2: Errors with time. Errors are counted when at least one of the REWS heights had an error.

The timing of outages and errors is shown in Figure 7.2. Outages are concentrated in the beginning of the measurement campaign. Outages were caused by occasional failure of the power supply, which has been resolved by Ecofys. The outages could be resolved in future measurement campaign and can be considered as random with respect to meteorological conditions. Therefore, these times have not been considered for further error/outages analysis. The figure shows that is

never the case that error 9998 and 9999 occur simultaneously at any of the REWS heights.

In order to understand whether errors are causing delays in the power performance measurements, the errors have been shown per wind speed in Figure 7.3, for relevant wind speed for the power performance test, with a wind speed above cut-in wind speed. The errors hardly cause any delay for the power performance measurements, because the errors occur at wind speeds that occur frequently. Therefor further analysis of the errors for power performance measurements is not needed. However, for so called "greenfield" measurements, to estimate the wind resource at a location, it can be important to understand more about the errors, some extra analysis therefore are included in Section F.
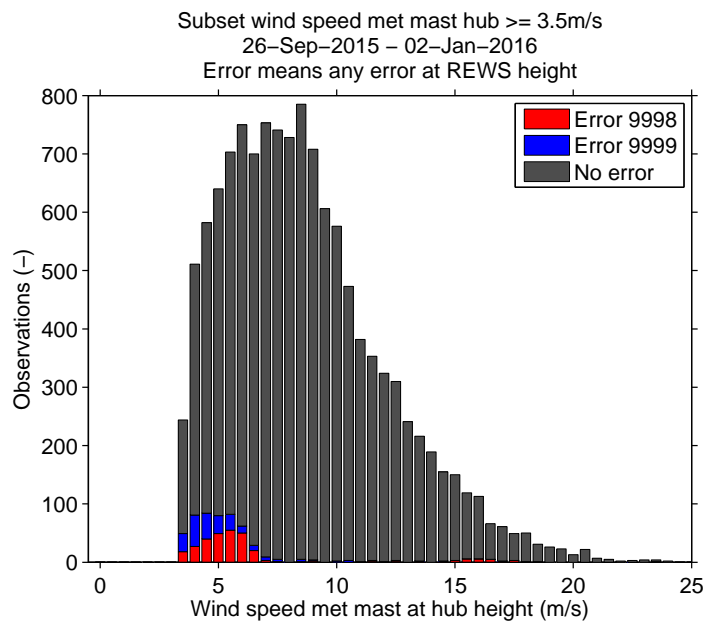
Figure 7.3: Error- and non-error observations per wind speed. For wind speeds relevant for the power performance test.

Chapter 8

Discussion & conclusion

For each research question the answers are provided, after which recommendations based on the research question are given. Thereafter limitations of the research and suggestions for future research are provided.

8.1 Answers on research questions and recommendations

1. *What are the site conditions during the measurement campaign?*

   The site conditions during the measurement campaign were favorable for power performance testing and enough data could be collected as was expected for these winter months. The prevailing wind direction was from the undisturbed sector and enough data was available for each 0.5 m/s wind speed bin.

   Recommendations (part 1)

   - The results of this study can be generalized for sites with non-complex terrain and multi-megawatt turbines with a hub height of approximately 100 meter and a rotor diameter of 100 meter. At this site there was a wind shear of approximately 0.2 which is typical for these type of sites with grassland.

2. *How well do the Lidar measurements compare to measurements of sensors at the meteorological mast?*

   The Lidar measures the wind speed according to Norswind standards at both measurement heights where the meteorological mast performs measurements too, at hub height and lower tip height of the wind turbine.

   The air density calculated using sensors at the Lidar are show correlation with the meteorological mast that is good enough for power performance testing. Even though there is scatter, the influence of the wind speed measurements that are accounting to the third power for energy in the wind are having a much larger influence than the air density.

The Lidar measures the wind direction either very well or sometimes with a error of 180 degrees. The wind direction measurement of the Lidar is dependent on its meteorological station.

Turbulence intensity figures of the Lidar and meteorological mast vary greatly, even when only looking at wind speeds higher than 3.5 m/s (here the cut-in wind speed).

Recommendations (part 2)

- The Lidar could be valuable to measure the power performance of wind turbines, because wind speed measurements of the Lidar show high correlations with those of the meteorological mast (and the Lidar was compliant to Norsewind standards). The mobile measurements can give added insights in the power performance of wind turbines at the whole site of a wind farm.

- For power performance testing, the meteorological station can be kept located at the Lidar because wind direction can be corrected for using wind turbine SCADA data.

- For green field measurements it is recommended to position the meteorological station in the undisturbed flow. A power generator, for example, providing electricity to the Lidar could better be positioned away from the Lidar or the meteorological station could be positioned on top of the generator. Using that approach, the wind direction offset of 180 degrees would not occur or at leas occur less frequently.

- It is not possible to obtain inner envelope filtering using the Lidar that is equal to a meteorological mast, because the turbulence intensity measurements are having a large scatter. For testing operational wind turbines, it is therefor recommended to either keep this in mind or to compare inner plus outer envelope conditions (thus all conditions allowed in the IEC power performance standard). For wind turbines where the power performance contract can be negotiated still, an option might be included where turbulence intensity measured by a Lidar would be approved too.

3. *How large is the relative difference of annual energy production calculations between measuring with a meteorological mast and measuring with a Lidar? What are the causes for that difference?*

The small difference in wind speed measurements have a large impact on AEP calculations. For this measurement campaign the difference in AEP was 2.5 % for a Rayleigh wind speed distribution with a mean annual wind speed of 7 m/s. These differences in AEP was clearly visible between the two wind turbines tested. Wind turbine E01 performed 6 percent worse than wind turbine E02 for a Rayleigh wind speed distribution with a mean annual wind speed of 7 m/s. Differences in AEP calculations were caused by differences in wind speed measurements while air density measurements were measured well enough and showed to have a fairly small impact.

Recommendations (part 3)

- Power performance measurements using a Lidar and using a meteorological mast should not be compared directly. However, comparing the performance of two wind turbines using either Lidar measurements or meteorological mast measurements can be valuable.

- It can be valuable to check the performance of wind turbines during operation. With appropriate measurements, malfunctioning can be found. This knowledge can be used for improving current performance, or for lessons learned for future projects. The wind turbine manufacturer was informed about the difference in power power performance of the two tested wind turbines. The manufacturer confirmed to check the wind turbine parameters (no results of the check were available during writing this report).

4. *How much does the scatter around the power curve reduce when applying corrections for rotor equivalent wind speed and veer? And what is the difference in calculated annual energy production?*

The rotor equivalent wind speed and hub height wind speed measured using the Lidar showed large similarities. For the rotor equivalent wind speed calculation, the wind speeds close to hub height have a larger impact than those far away from the hub height. For the wind turbines under study, 72 % of the impact came from the measurement heights 21 meter above to 21 meter below hub height. The average difference in wind speed over this section was relatively small. With the larger wind turbines at the moment having a rotor diameter of for example 150 meter, the effect becomes much more significant. The measurement campaign was held in flat terrain, thus at complex terrain the rotor equivalent wind speed might differ more. The advantage of including rotor equivalent wind speed is that the uncertainty of the energy in the wind over the rotor plane is better represented than when only measuring at hub height, which also reduced the scatter in the power curve compared calculations using the Lidar wind speed at hub height. The scatter around the power curve reduced when using the rotor equivalent wind speed, compared to Lidar hub height wind speed. A disadvantage is that when calculating the AEP, also the rotor equivalent annual wind speed should be known. This requires measurement at multiple heights and also adjusting the wind speed towards different turbine types.

The calculated AEP showed a difference of 0.5 percent for a Rayleigh wind speed distribution with a mean annual wind speed of 7 m/s which was used for both the hub height wind speed distribution as the rotor equivalent wind speed distribution.

In comparison with rotor equivalent wind speed, veer correction showed less effect on AEP and scatter. The difference in AEP was 0.2 percent using a Rayleigh wind speed distribution with 7 m/s mean annual wind speed and the effect on scatter was negligible.

Recommendations (part 4)

- For sites with flat terrain with grassland and wind turbines with a hub height and rotor diameter of approximately 100 meter, it is not recommended to use rotor equivalent

wind speed calculations correction for annual energy production forecasting. The reason being that uncertainty does not decrease significantly and for each turbine type, a new rotor equivalent wind speed needs to be calculated, and a rotor equivalent mean annual wind speed needs to be approximated for annual energy production calculations. However the added value could become larger for more complex terrains, for terrains with more vegetation or for sites with larger wind turbines. For power performance testing of operational wind turbines using a Lidar, the amount of extra needed calculations is less apparent than for annual energy production forecast. When in doubt whether the wind speed variation with height plays an important role on the power performance of a wind turbine it therefor might easily be calculated next to the regular calculations.

- If one applies rotor equivalent wind speed calculations, then we recommend to include veer correction too (even though veer correction did not show large impacts on annual energy performance calculations or reducing scatter). The calculation is straightforward and prevents having too high wind speeds as input for the rotor equivalent wind speed calculation. At sites with a significant change of wind direction with height it would not be fair to interpret the wind speed at each height as perpendicular to the rotor disc, because it would introduce an error that could easily be prevented.

5. *What percentage of time do inner-envelope conditions occur? And what is the annual energy production difference for inner- and outer- envelope conditions of the guaranteed power curve?*

The inner envelope conditions together with wind speeds above cut-in wind speed occurred only during 24 percent of the time. A part of the data rejection was caused by the conditions needed for an IEC power performance test and wind speeds above cut-in wind speed, after which only 57 percent of the total measurement time was still available. Within the IEC compliant power performance test conditions, wind shear and turbulence intensity restrictions in the power curve guarantee caused the rest of the data filtering.

The power performance for inner-envelope conditions was approximately 0.8 percent higher than when including all IEC compliant conditions, for a Rayleigh wind speed distribution with a 7 m/s mean annual wind speed.

Recommendations (part 5)

- For power performance guarantee negotiations it is advised to calculate beforehand what percentage of time the inner envelope conditions are expected to occur as well as to think of the performance during the other moments. For example one can ask for one power curve valid for inner-envelope conditions together with one that is valid for the rest of the conditions within the IEC compliant measurements. Another option could be to limit the restrictions for inner-envelope conditions, for example by including a rotor equivalent wind speed approach and in the future possibly a turbulence intensity corrected power curve.

6. *Are errors and outages of the Lidar systematically occurring during certain meteorological conditions?*

When the Lidar is unable to measure the wind speed and wind direction, this is almost always at low wind speeds, for example when there is fog.

Recommendations (part 6)

- For power performance testing, no extra time should be reserved for Lidar measurement campaigns compared to meteorological mast measurement campaigns. The reason is that errors almost never occur at high wind speeds (which occur less often than lower wind speeds).

- For greenfield measurements, care should be taken with errors, an increased amount of errors enlarges the overestimation of the average wind speed, because errors occur most often during low wind speeds, for example during periods with fog.

8.2   Limitations and suggestions for future research

In this study we focused on the impact of rotor equivalent wind speed and veer, but it would also be valuable to analyze the influence of turbulence intensity in future research. The influence of turbulence intensity correction as suggested by Wagenaar and Eecen (2011) or IEC (2015) could be performed.

While this study focuses on flat terrain, it could also be valuable to perform similar studies for complex terrain and compare the impact of Lidar measurements on power performance testing for those conditions.

It could be valuable to continue the discussion on which measurement device is 'correct', because the cup anemometers and Lidars measure different properties (for example the point measurement approximation versus volume measurement). In the same line of thought it would be interesting to think on methods to validate a Lidar in a flow that has constant wind speed, for example in a valley where this was found using repositioning a meteorological mast so that it could be tested how well the Lidar measures when over constant wind speeds to exclude the effect of the 'point' versus volume measurements.

As this study showed, inner versus outer envelope conditions can show large differences in power performance of wind turbines. Therefor it could be valuable to further quantify factors influencing these differences and to continue establishing standard methodologies to increase the insight on power performance of wind turbines under all conditions.

Bibliography

Antoniou, I., Pedersen, S. r. M., and Enevoldsen, P. B. (2009). Wind Shear and Uncertainties in Power Curve Measurement and Wind Resources. *Wind Engineering*, 33(5):449–468.

Bingöl, F., Mann, J., and Foussekis, D. (2009). Conically scanning lidar error in complex terrain. *Meteorol. Zeitschrift*, 18(2):189–195.

Courtney, M., Wagner, R., and Lindelöw, P. (2008). Testing and comparison of lidars for profile and turbulence measurements in wind energy. In *IOP Conference Series: Earth and Environmental Science*, volume 1, page 012021. IOP Publishing.

Danielian, R., Jorgensen, H., Mikkelsen, T., Mann, J., and Harris, M. (2006). Surface-layer wind and turbulence profiling from lidar: Theory and measurements. In *European Wind Energy Conference*.

Dupont, E., Lefranc, Y., Soulier, L., and Koulibaly, D. (2012). Detailed analysis of uncertainty reduction on power curve determination using lidar measurements. *Proceeding of EWEA2012, Copenhagen (2012)*, (April):16–19.

EWEA (2009). Wind energy - the facts: a guide to the technology, economics and future of wind power. European Wind Energy Association.

Garrard Hassan (2010). Assessment of the energy production of the proposed Zuidlob wind farm. Technical report. Document 103116/DR/01. The report is confidential except for the park layout.

Goossens, S. and Hough, J. (2015). Scope of Work: Princess Alexia Wind Farm LiDAR measurement. Technical report. Document id: NL.NZL.LM01CA1. Internal report.

GWEC (2014). Global wind report. Technical report.

Hansen, M. O. (2015). *Aerodynamics of wind turbines*. Routledge.

Hasager, C., Stein, D., Courtney, M., Peña, A., Mikkelsen, T., Stickland, M., and Oldroyd, A. (2013). Hub Height Ocean Winds over the North Sea Observed by the NORSEWInD Lidar Array: Measuring Techniques, Quality Control and Data Management. *Remote Sens.*, 5(9):4280–4303.

Hieronimus, J. (2015). Wind speed measurements in an offshore wind farm by remote sensing. a comparison of radar satellite terrasar-x and ground-based lidar systems. Msc. thesis.

IEA (2013). Technology roadmap wind energy. International Energy Agency.

IEA (2015). *Key world energy statistics*. International Energy Agency.

IEC (2005). 61400-12-1 Wind turbines–Part 12-1: Power performance measurements of electricity producing wind turbines. *IEC-TC88 Maint. Team MT12-1*. International Electrotechnical Commission.

IEC (2013). 61400-12-1 Wind turbines–Part 12-1 Ed 2 Draft: Power performance measurements of electricity producing wind turbines. *IEC-TC88 Maint. Team MT12-1*. International Electrotechnical Commission.

IEC (2015). 61400-12-1 Wind turbines–Part 12-1 Ed 2 Draft CDV version 4: Power performance measurements of electricity producing wind turbines. *IEC-TC88 Maint. Team MT12-1*. International Electrotechnical Commission.

ISO (1975). International standard 2533 - standard atmosphere. *ISO*, 2533:1975. International organization for standardization.

Jaynes, D. W., Manwell, J. F., McGowan, J. G., Stein, W. M., and Rogers, A. L. (2007). Mtc final progress report: Lidar. *Renewable Energy Research Laboratory, Department of Mechanical and Industrial Engineering, University of Massachusetts*.

Justus, C. (1978). Winds and wind system performance [wind power]. *Solar Energy Series (USA)*.

KNMI (2016). Hourly data from the knmi meteorological station lelystad. Technical report. Royal Netherlands Meteorological Institute.

Lewis, A. (2016). Telephone interview. February 22, 2016. ZephIR.

Lindelöw-marsden, P. (2009). *Uncertainties in wind assessment with LIDAR*, volume 1681.

Mann, J., Cariou, J.-P., Courtney, M. S., Parmentier, R., Mikkelsen, T., Wagner, R., Lindelöw, P., Sjöholm, M., and Enevoldsen, K. (2008). Comparison of 3d turbulence measurements using three staring wind lidars and a sonic anemometer. In *IOP Conference Series: Earth and Environmental Science*, volume 1, page 012012. IOP Publishing.

Mann, J., Peña, A., Bingöl, F., Wagner, R., and Courtney, M. (2010). Lidar scanning of momentum flux in and above the atmospheric surface layer. *Journal of Atmospheric and Oceanic Technology*, 27(6):959–976.

Manwell, J. F., McGowan, J. G., and Rogers, A. L. (2010). *Wind energy explained: theory, design and application*. John Wiley & Sons.

Pena, A., Hasager, C. B., Gryning, S.-E., Courtney, M., Antoniou, I., and Mikkelsen, T. (2009). Offshore wind profiling using light detection and ranging measurements. *Wind Energy*, 12.

RES (2014). Project Cyclops: the way forward in power curve measurement? Technical report. Renewable Energy Systems Ltd.

Smith, D. A., Harris, M., Coffey, A. S., Mikkelsen, T., Jø rgensen, H. E., Mann, J., and Danielian, R. (2005). Wind lidar evaluation at the Danish wind test site in Høvsøre. *Wind Energy*, 9(1-2):87–93.

Thøgersen (2005). Modelling of the variation of air density with altitude through pressure, humidity and temperature. Technical report. WindPRO reference manual.

TU Delft (2016). Wind field modeling for wind turbine design calculations. `http://www.lr.tudelft.nl/index.php?id=28670&L=1`. Online; accessed January 11, 2016.

Wächter, M., Gottschall, J., Rettenmeier, A., and Peinke, J. (2009). Power curve estimation using lidar measurements. In *Proceedings of the EWEA European Wind Energy Conference*.

Wagenaar, J. W. and Eecen, P. J. (2011). Dependence of Power Performance on Atmospheric Conditions and Possible Corrections. *Eur. Wind Energy Conf.*, (March):14–17.

Wagner, R., Cañadillas, B., Clifton, A., Feeney, S., Nygaard, N., Poodt, M., Martin, C. S., Tüxen, E., and Wagenaar, J. W. (2014). Rotor equivalent wind speed for power curve measurement – comparative exercise for IEA Wind Annex 32. *J. Phys. Conf. Ser.*, 524:012108.

Wagner, R., Courtney, M., Gottschall, J., and Lindelöw-Marsden, P. (2011). Accounting for the speed shear in wind turbine power performance measurement. *Wind Energy*, 14(8):993–1004.

Weitkamp, C. and Wandinger, U. (2005). Lidar: Range-resolved optical remote sensing of the atmosphere. ISBN 0-387-40075-3.

Wessels, R. H. J. (2015). An experimental study into accuracy of novel techniques in Power Curve verification. Master thesis report.

Westerhellweg, A., Canadillas, B., Beeken, A., and Neumann, T. (2010). One year of lidar measurements at fino1-platform: Comparison and verification to met-mast data. In *Proceedings of 10th German Wind Energy Conference DEWEK*, pages 1–5.

Wharton, S. and Lundquist, J. K. (2012). Atmospheric stability affects wind turbine power collection. *Environmental Research Letters*, 7(1):014005.

WICO (2015). Power curve measurement at the wind turbine. WIND-consult report WICO 247LKC14/01.

ZephIR (2015a). ZephIR 300 Data Analysis - A guide on analyzing the data from your ZephIR 300. V1.0.

ZephIR (2015b). ZephIR 300 Siting and Deployment Guide - A guide on siting and deploying your ZephIR 300. V1.0.

ZephIR (2015c). ZephIR 300 Technical specifications. `http://www.zephirlidar.com/support/tech-specs/`. Online; accessed November 10, 2015.

Appendix A

Velocity azimuth display

In this section Equation 2.4 from Section 2.1.2 is derived.

A.1   Line of sight wind velocity

For a given wind velocity vector (u, v, w), the line of sight velocity can be deducted when the azimuth angle θ and the elevation angle ϕ are known.

The horizontal component of the line of sight velocity $u_{LOS,hor}$ can be deducted from the wind speed component to the north u and to the south v, using the azimuth angle θ (Figure 2.6).

$$u_{LOS,hor} = v\cos(\theta) + u\sin(\theta) \tag{A.1}$$

The vertical component of the line of sight velocity $u_{LOS,ver}$ equals the vertical component of the wind speed.

$$u_{LOS,ver} = w \tag{A.2}$$

The line of sight velocity can be deducted from its horizontal and vertical component and the elevation angle.

$$u_{LOS} = u_{LOS,hor}\cos(\phi) + u_{LOS,ver}\sin(\phi) \tag{A.3}$$

$$u_{LOS} = u\sin(\theta)\cos(\phi) + v\cos(\theta)\cos(\phi) + w\sin(\phi) \tag{A.4}$$

A.2   Velocity azimuth display reading

The wind velocity vector (u, v, w) can be obtained from the line of sight wind speed when scanning multiple azimuth angles. When the line of sight wind speed is plotted against the azimuth

angle, the velocity azimuth display is obtained as was shown Figure 2.7. The scatter can be fitted against a cosine function.

$$u_{LOS} = a + b\cos(\theta - \theta_{max}) \tag{A.5}$$

Where θ_{max} is the azimuth angle where the highest line of sight velocity is observed, also called the phase shift of the cosine function.

Using the fitted cosine function (Equation A.5), the wind speed and wind direction can be found (Figure 2.7). The offset a equals the part that is independent of the azimuth angle θ, which is the vertical wind speed $w\sin(\phi)$. The maximum of the fitted cosine function shows the direction where the line of sight velocity is at its maximum, thus to which direction the wind is blowing. The angle there is defined as θ_{max}. Using the same trigonometry as in Section A.1, the wind speed can be found in South-North and West-East direction as was given in Equation 2.4.

Appendix B

Wind conditions since installation of meteorological mast

Figure B.1 shows meteorological conditions at the site since the meteorological mast was installed.

(a) Wind speed distribution

(b) Wind rose
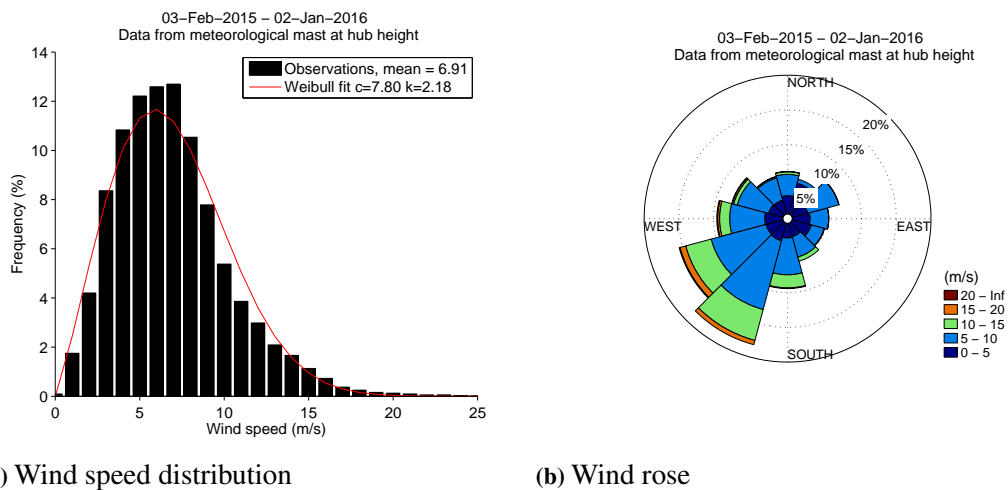
Figure B.1: Wind conditions at the site since the installation of the meteorological mast.

Appendix C

Air temperature, air pressure, relative humidity
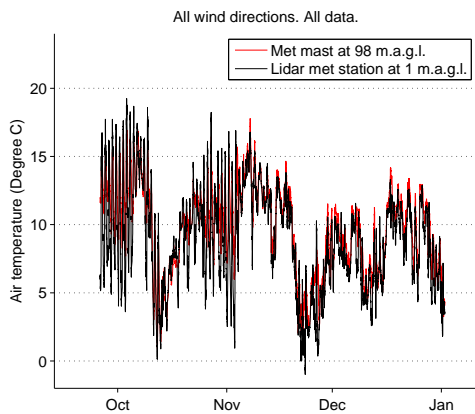
(a) Lidar data not corrected to height
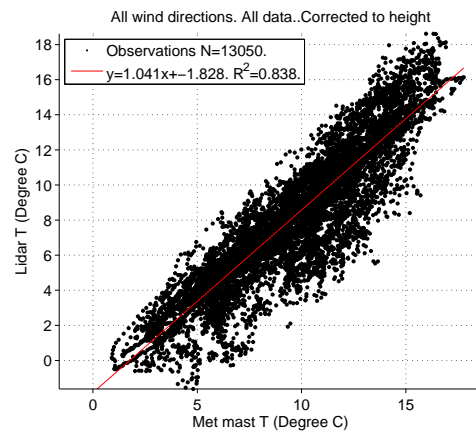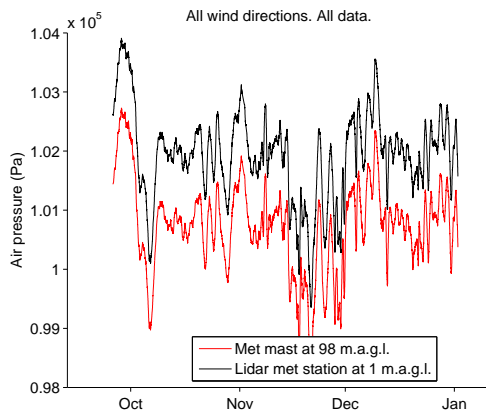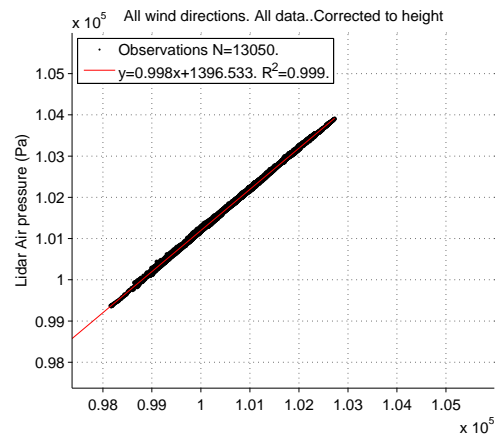

(b) Lidar data not corrected to height
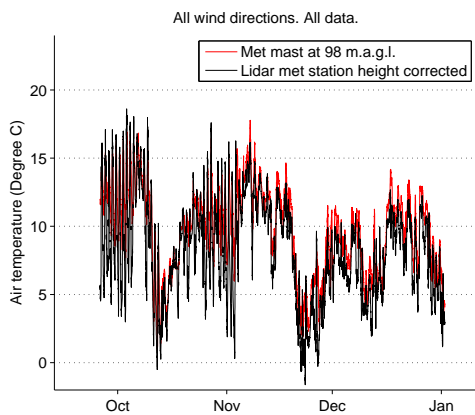
(c) Lidar data corrected to height
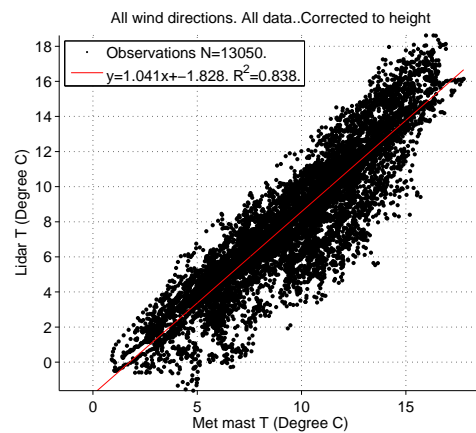
(d) Lidar data corrected to height

Figure C.1: Air temperature.

(a) Lidar data not corrected to height

(b) Lidar data not corrected to height
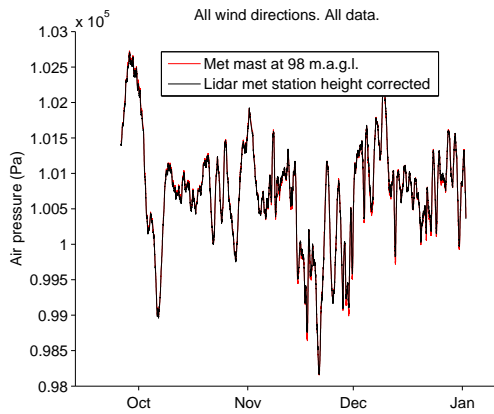
(c) Lidar data corrected to height
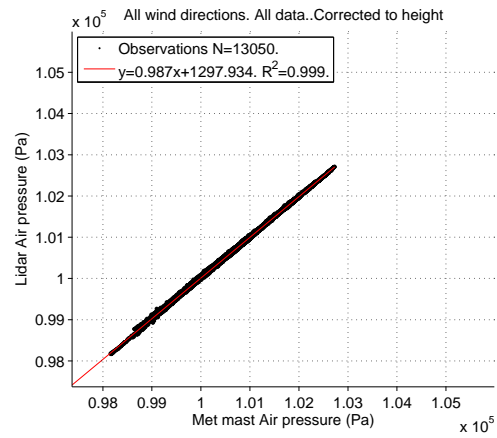
(d) Lidar data corrected to height

Figure C.2: Air pressure.
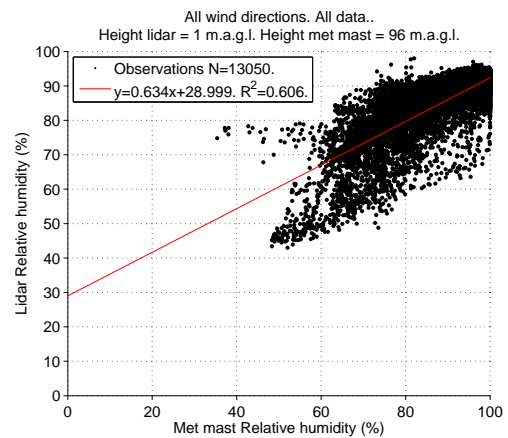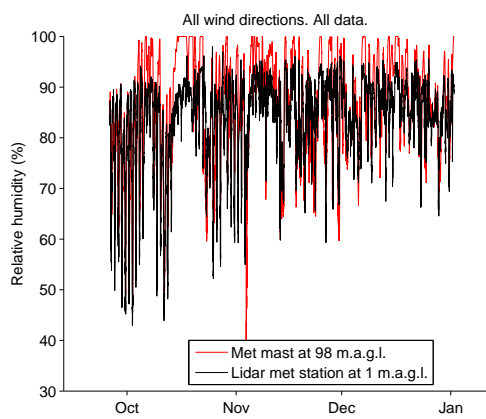
Figure C.3: Relative humidity.

Appendix D

Cut-out hysteresis

Cut-out hysteresis loops were the wind turbine did not get back to rated power after a cut-out wind speed was reached was excluded from the data as (Section 3.5.1). Hysteresis loops in the cut-out algorithm as described in Section 3.5.1 have been checked for in Figure D.1 and Figure D.2. All data is plotted where the meteorological mast measured a hub height wind speed of at least 23 m/s in the past 24 hours. by looking at all data where in the last 24 hours the hub height wind speed measured by the meteorological mast was higher than the cut-out wind speed minus 2 m/s. Drops to zero power have to be analyzed and excluded when the wind speed was larger than cut-in wind speed.
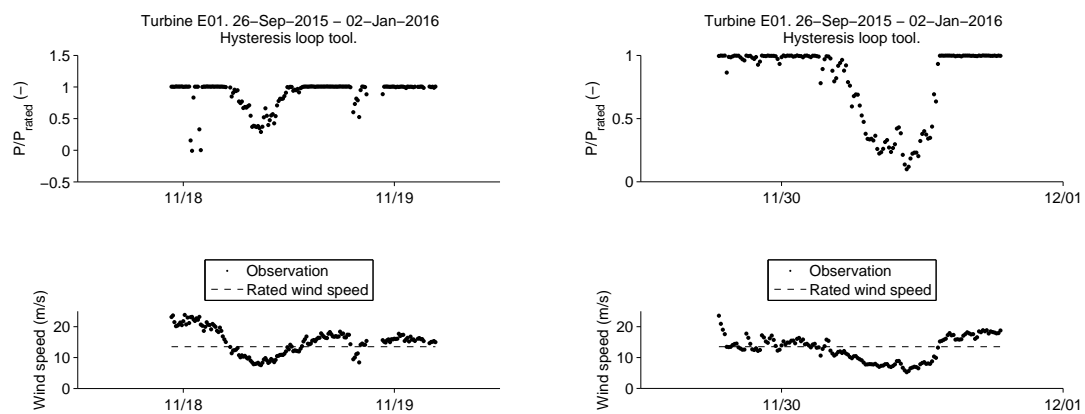
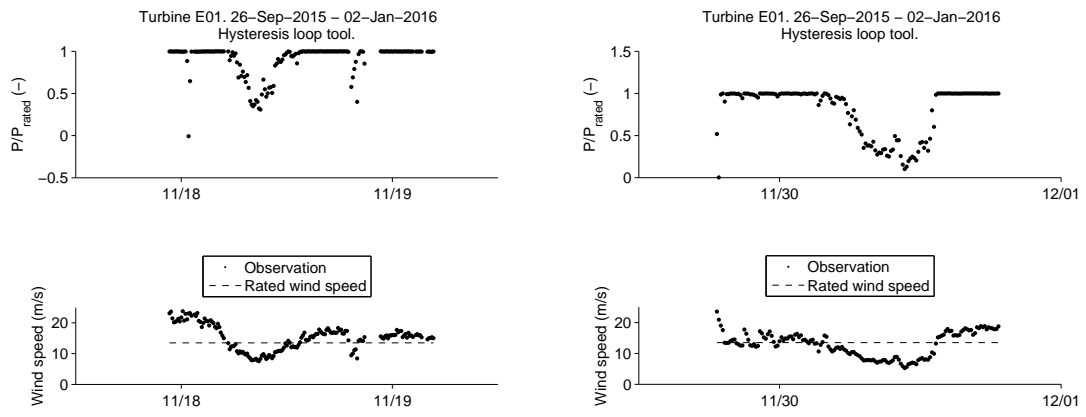**Figure D.1:** Cut-out hysteresis loops of wind turbine E01.

**Figure D.2:** Cut-out hysteresis loops of wind turbine E02.

Appendix E

Wind profile

The wind profile as measured with the Lidar wind speeds is depicted in Figure E.1. Wind speed was taken from the Lidar, and wind direction from meteorological mast.

When focusing on the wind directions where wind turbine E01 and wind turbine E02 are positioned, then the wake of the turbines can is seen in Figure E.2. This method was applied by Goossens and Hough (2015) for Sodar measurements.

When normalizing to the highest average wind speed per wind sector.
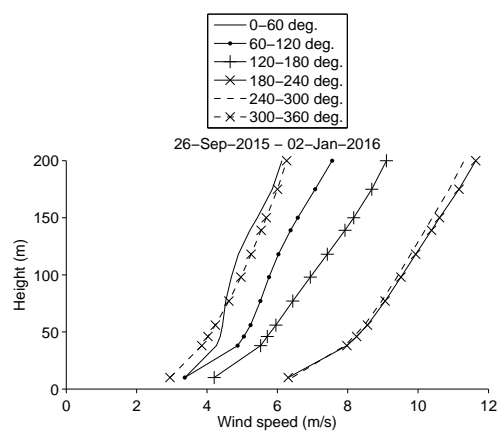
Figure E.1: Wind profile filtered for wind direction.
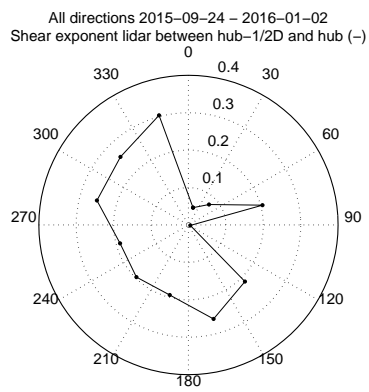
(a) E01

(b) E02
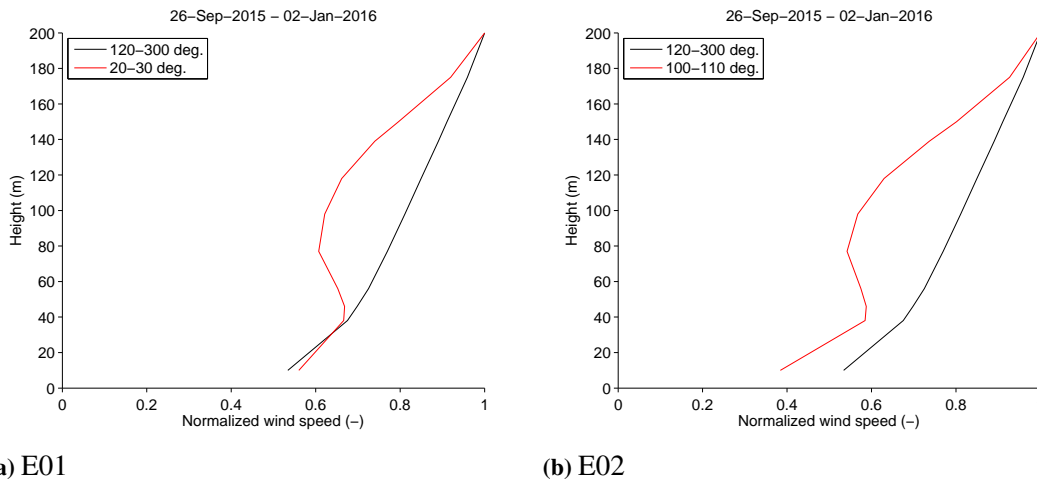
Figure E.2: Wake effect of wind turbine E01 and E02 on the wind profile at the location of the Lidar. The wind speed is normalized to the sector average wind speed at 200 meter.

Figure E.3 shows the mean wind speed with height for different wind directions. The direction 0-60 degrees is the direction of wind turbine E01 which is closest by and of which the influence on the wind profile from can be seen. Figure E.4 shows the shear exponent calculated using Equation 3.8.
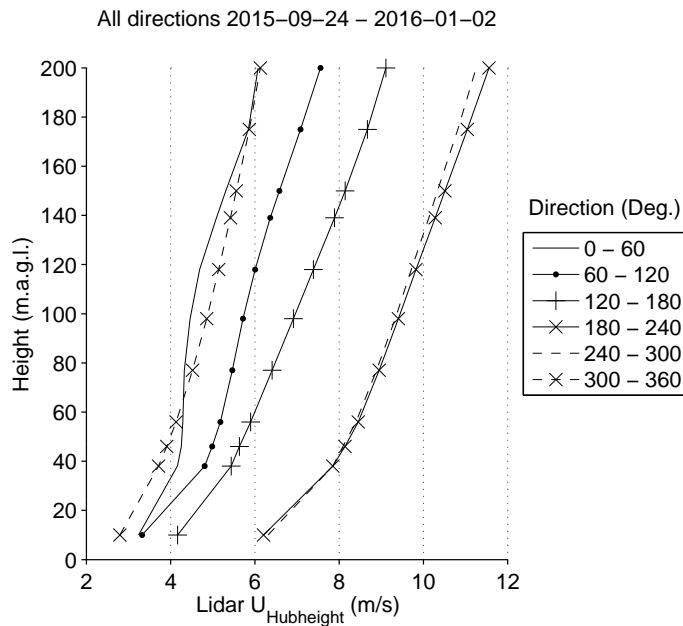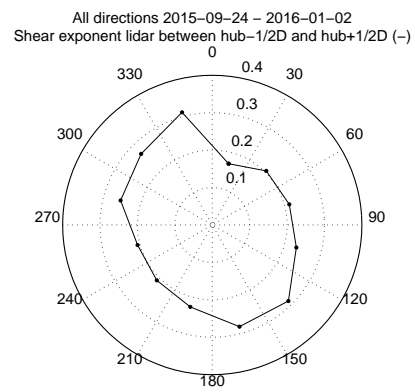

Figure E.3: Mean wind speed with height measured by the lidar for different wind directions measured by the meteorological mast

All directions 2015−09−24 – 2016−01−02
Shear exponent lidar between hub−1/2D and hub (−)

All directions 2015−09−24 – 2016−01−02
Shear exponent lidar between hub−1/2D and hub+1/2D (−)

**(a)** Hub-1/2D to Hub   **(b)** Hub-1/2D to Hub+1/2D

Figure E.4: Average shear exponent for different wind directions using lidar measurements.

Appendix F

Lidar outages and error ananalysis for greenfield measurements

When a Lidar is used for so called "greenfield" measurements, to estimate the wind resource at a site, different criteria are needed than for a power performance test. For a power performance test it is important to acquire a minimum amount of data points per wind speed bin. Whereas for a greenfield measurement, it is important to estimate the average wind speed, hence, to know whether errors cause an under or over prediction of the wind speed.

Figure F.1 shows that errors are occurring at low wind speeds. Therefor, an increasing amount of errors during a measurement campaign would lead to higher estimated wind speeds for a Lidar ZephIR 300 measurement campaign.
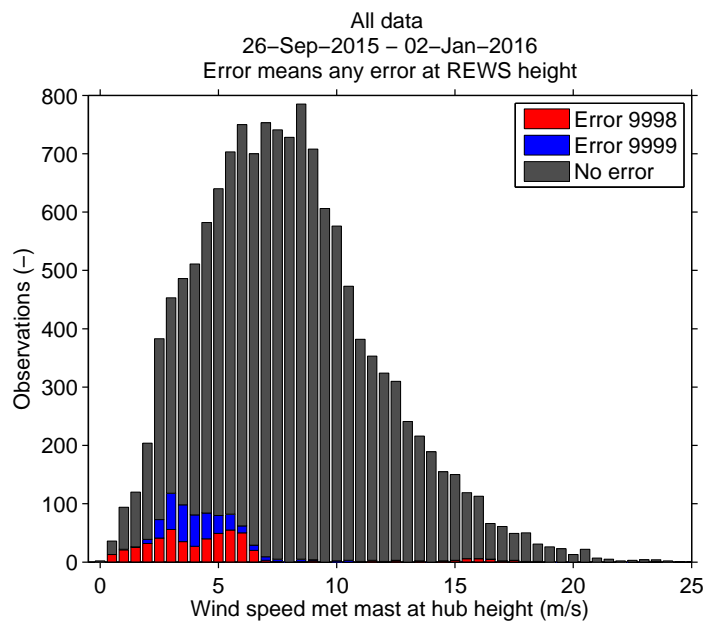
Figure F.1: Errors and non-error observations, per wind speed relevant for wind resource estimation shown as stacked bar chart. Equal to Figure 7.3, but now also including wind speeds below cut-in wind speed.

The error analysis reveals that the occurrence of error code 9998 (atmospheric conditions) increases with height as shown in Figure F.2, which makes sense when fog would be present. For error code 9999, this effect is not clear (code 9999: "partial obscuration of the ZephIR window, or significant interference with the laser beam at the specified height" (ZephIR, 2015a)).

To check whether fog is a plausible explanation for error, the timing of these errors is shown in Figure F.3. This error occurs most often during the night and fog was often also signaled at the KNMI meteorological station in Lelystad, where the signal 'Fog' has been analyzed which could take the value 0 for no occurrence or 1 for occurred during the preceding hour and/or at the time of observation (KNMI, 2016). It can be concluded that error 9998 most often seems te be caused by fog. With fog mostly occurring with low wind speeds, this increases the confidence that when the errors increase, the overestimation of the mean wind speed increases.
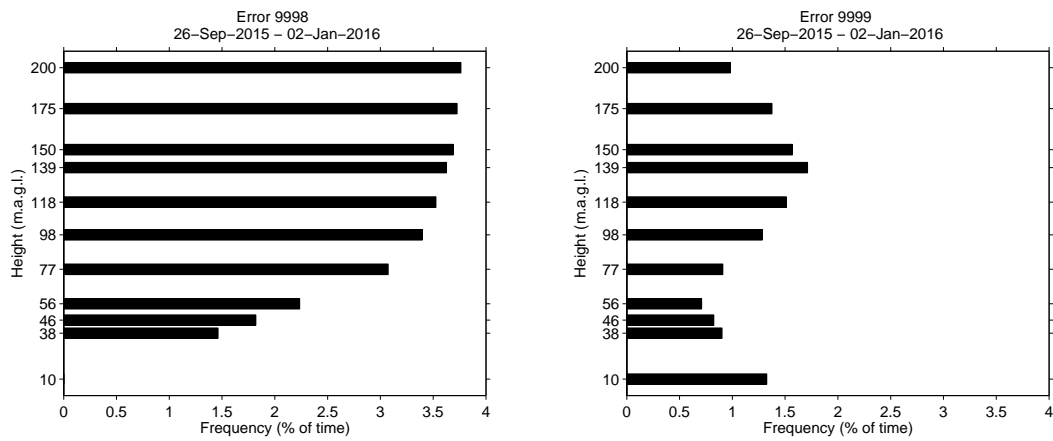
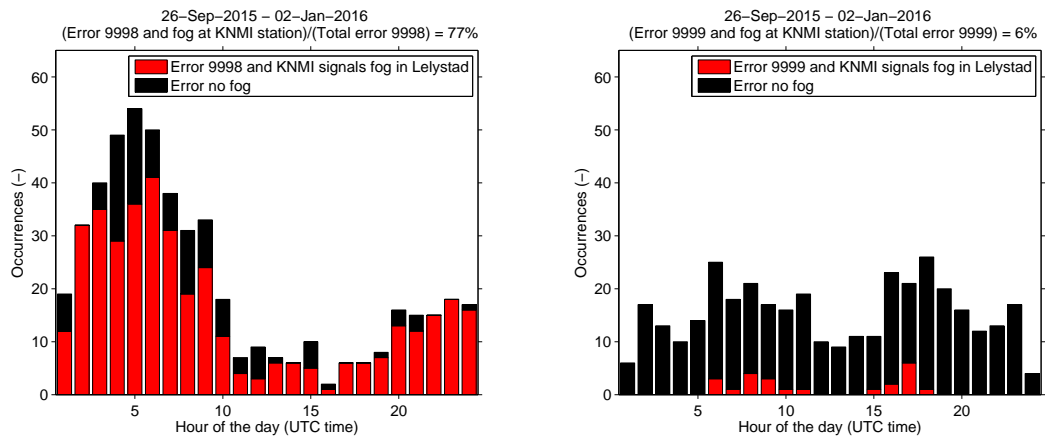**Figure F.2:** Lidar errors with height.

Figure F.3: Fog analysis showing Lidar Error 9998 occurs often when fog is signalled at the KNMI weather station Lelystad, while this is not the case for Lidar error 9999.